Droplet Control Technologies for Microfluidic High Throughput Screening (μHTS)

Muhsincan Sesen,[a] Tuncay Alan,[a] and Adrian Neild*[a]

Received Xth XXXXXXXXXX 20XX, Accepted Xth XXXXXXXXX 20XX
First published on the web Xth XXXXXXXXXX 200X
DOI: 10.1039/b000000x

The transition from micro well plate and robotics based high throughput screening (HTS) to chip based screening has already started. This transition promises reduced droplet volumes thereby decreasing the amount of fluids used in these studies. Moreover, it significantly boosts throughput allowing screening to keep pace with the overwhelming number of molecular targets being discovered. In this review, we analyse state-of-the-art droplet control technologies that exhibit potential to be used in this new generation of screening devices. Since these systems are enclosed and usually planar, even some of the straightforward methods used in traditional HTS such as pipetting and reading can prove challenging to replicate in Microfluidic High Throughput Screening (μHTS). We critically review the technologies developed for this purpose in depth, describing the underlying physics and discussing the future outlooks.

1 Introduction

Microfluidics is the study of fluid flow at the sub-millimetre scale. Over recent years, microfluidics has grown to be a prominent research field owing to the wide spectrum of potential applications it offers. The field of microfluidics has attracted researchers from physics, chemistry, biology and engineering and has quickly become an important interdisciplinary research topic. What microfluidics offers is simple yet highly beneficial: nanolitre scale fluid consumption with minimal operation times. Standard laboratory procedures such as pipetting, mixing, centrifugation and incubation require expensive and bulky equipment, large amounts of consumables and high maintenance laboratories while being relatively slow processes. Microfluidics promises to outperform such laboratory procedures on disposable, inexpensive microchips; thus the concept of lab-on-a-chip (LOC) devices.

What makes LOC devices so attractive is that they offer sample and reagent reduction, high throughput analysis, faster reaction times, higher sensitivity and overall cost reduction. Microfluidics, today, finds numerous applications in a wide variety of fields such as forensic DNA analysis [1], diagnostics [2,3], organs-on-chip [4,5], cell biology [6], next generation sequencing [7,8], environmental studies [9–11], space exploration [12], energy [13] and nutrition [14,15]. It has also opened up opportunities to perform brand new types of experiments allowing rare-cell detection [16] and giving rise to microfluidic reactors [17] for the discovery of new chemical entities [18].

Fluid flow characteristics at the microscale are substantially different to those of its macroscale counterpart. As length scales are decreased, body forces like gravity lose their significance and give way to surface forces such as interfacial tension and viscous forces. In microchannels, the flows are viscosity dominated rather than inertia, therefore the laminar flow regime is relevant to microfluidics. External pumps, valves and actuators need to be redesigned for microfluidic channels measuring hundreds of micrometres or less. These dissimilarities are sometimes advantageous but more often they have posed significant challenges in the design process. This has lead researchers to utilise various methods for fluid flow manipulation such as membrane deformation [19,20], centrifugal forces [21] and electrokinetic pumps [22]. Moreover, in order to manipulate particles and cells in microchannels [23,24], there's been extensive research around acoustic [25–27], magnetic [28] and electrical separation techniques [29,30] as well as inertial microfluidics [31] and hydrodynamic methods such as deterministic lateral displacement [32]. Between the last two decades, microfluidics was born, grown and it has already revolutionised many sectors in the medical industry [33] such as single cell 'omics' [34] and advanced the development of hand-held, affordable point-of-care diagnostic devices [35,36]; at the same time, it remains a young and growing field which continues to evolve as a research subject.

A subset of microfluidics is the study of multiphase (segmented) flows. Monodisperse droplets of nL to fL volumes can be generated in an immiscible carrier liquid at rates exceeding 20kHz [37,38], allowing exhaustive studies to be carried out in rapid succession in microfluidic devices. Often

[a] *Department of Mechanical and Aerospace Engineering, Monash University, Clayton, VIC 3800, Australia. E-mail: adrian.neild@monash.edu; Tel: +61 3 990 54655*

† Electronic Supplementary Information (ESI) available. See DOI: 10.1039/b000000x/

termed droplet or digital microfluidics, it offers chemical and physical isolation of droplets to avoid cross-contamination because such droplets are segmented by the immiscible carrier fluid. These systems promise accurate control of droplet volumes, single-cell analysis capabilities, repeatable and reliable droplet manipulation, high throughput capability and automation. Its applications encompass protein crystallisation[39,40], chemical and biological assays[41,42] and inorganic chemistry [43]. The reader is referred to recent reviews on various assays, screens and studies enabled by droplet microfluidics[44] as well as its applications in drug discovery, transcriptomics and molecular genetics[45].

Each droplet can be identified as a miniature reaction compartment. Single cells may be encapsulated within these droplets and exposed to various chemicals or external excitation such as ultraviolet (UV) light or thermal cycling. If microfluidic droplets are formed using a cell culture as the dispersed phase, the number of cells trapped within each droplet agrees with a Poisson distribution[46]. Efforts to improve the probability of trapping one cell per droplet include squeezing particles into a single file to achieve ordered formation[47], utilising a high aspect ratio entrance channel so that cells arrange themselves in an equally spaced manner due to inertial forces [48] and Dean-coupled inertial ordering of cells in curved microchannels[49]. A recent review focussed on the state-of-the-art for single cell encapsulation and exceeding the limitations set by Poisson statistics[50]. High droplet formation rates and the encapsulation of single cells within droplets allow very large screens to be processed with low volumes of fluids used to find unique cell types in a heterogeneous population such as antibiotic-resistant bacteria[51] or to carry out a directed evolution experiment[52]. Applications of single-cell analysis in droplet-based microfluidics range from gene expression and cytotoxicity to digital polymerase chain reaction (dPCR) and antibody secretion studies[44,53,54].

It has been more than a decade since visionaries suggested that such two phase LOC devices, especially digital microfluidic devices, could revolutionise high throughput screening (HTS) technology[55–58]. HTS is the widespread method for early drug screening studies carried out by pharmaceutical companies. It is an empirical method to test disease-carrying targets (such as cells and proteins) against a library of compounds resulting in millions of combinations, in the hunt for a positive reaction. It has recently played a key role in the discovery of drugs to fight diabetes, cancer and HIV[59].

HTS has gone through its own miniaturisation period and evolved into ultraHTS (uHTS) by increasing the number of wells on micro plates a hundred-fold reducing the amount of fluids used and time spent. This is now estimated to save US$130 million and 9 months for the commercialisation of one drug[60]. Nevertheless, it costs companies approximately US$1.5 billion and 10 years[59,61] to bring a drug to the market with the bottleneck being reagent volume[44]. It is thought that miniaturisation of uHTS has reached its limits, which are imposed by evaporation in open systems[58,62] and the accuracy of robotic dispensing.

A strong candidate for replacing HTS technology is the usage of droplet microfluidics since they can offer further miniaturisation with increased throughputs, lower costs and no evaporation issues[63]. In addition, reactions could substantially benefit from this miniaturisation since highly concentrated samples yield faster reactions. The volume of a compartment can be shrunk by up to 7 orders of magnitude[44] in droplet microfluidic systems, consequently, the concentration of single molecules or cells significantly increases within a given compartment boosting sensitivity in diagnostic assays.

Recent developments in droplet microfluidics[45], emerging techniques for single-cell RNA sequencing (scRNA-seq)[64] as well as off-the-shelf products and emerging companies[65] indicate that we are in the midst of this paradigm shift. To give a few examples; Dolomite Bio offers the RNA-seq system for scRNA-seq, especially the recently developed Drop-seq protocol[66], The Chromium ™ controller by 10x Genomics is another recent automated droplet microfluidic system capable of scRNA-seq. The QX200™ Droplet Digital™ PCR System by Bio-Rad encapsulates samples into droplets before thermal cycling to quantify target nucleic acids via optical detection.

There still exists several shortcomings associated with this paradigm shift[67], especially given the fact that droplet microfluidic systems are enclosed, planar and driven by continuous flow with high throughputs. Most systems do not go beyond generating a droplet library because even the most common and straightforward laboratory procedures such as pipetting and centrifugation can prove to be quite challenging when working with droplets in closed channels with rates up to tens of thousands per second. Indeed, the very rapidity of production, so perfect for tasks such as single cell analysis, poses real control problems for on-chip HTS. Therefore, droplet manipulation techniques have been extensively studied in the literature to advance existing methods.

The scope of this review encompasses pressure driven, closed channel, aqueous in oil droplet microfluidic systems and on-chip techniques exhibiting potential applications in HTS, therefore, equally prominent subjects such as droplet/bubble logic[68–71], multiple emulsions[72–76], chemical assaying[77] and electrowetting on dielectric (EWOD)[78–80] were excluded for a succinct review. Broader droplet microfluidics reviews[42,81–83] as well as specialised reviews looking at applications[84], cell encapsulation in droplets[50,53,54], drug discovery[45,67], analytical detection[77,85], droplet dynamics[86], formation[87,88] and sorting[89] have been carried out. Here, we thoroughly investigate the state-of-the-art droplet methods enabling HTS studies to be performed on LOC devices, in other words, pioneers of Microfluidic High Throughput Screening

(μHTS). These are supported by discussions on working principles, physics, cross-compatibility, further improvements and future directions.

2 Combinatorial Library

The power of HTS stems from its ability to screen multiple targets of alternate compositions at the same time, reducing the time for discovery, therefore, interfacing multiple reservoirs to a single chip to form a combinatorial library is extremely important. A combinatorial library is formed when a pool of chemicals (e.g targets) are mixed with another pool of chemicals (e.g reagents) where all the possible combinations are obtained. It's quite straightforward to attain a spatial barcoding using robotic pipettes to dispense into open well plates whereby desired sample combination can be sequentially deposited to specific locations. However, these aspects of HTS pose big challenges in closed, planar, continuous droplet microfluidic systems; a robust, versatile and cross-compatible microfluidic chip capable of generating a combinatorial library where droplets can be barcoded, tagged or sequentially introduced will certainly play a key role in the transition to μHTS.

Two main strategies are prevalent for keeping track of the chemical composition of each variant in the library; labelling and sequencing. Labelling involves mixing in a unique identifier tag with every chemical used in the library. This could be achieved by using nucleic acid sequences[66,90,91] or fluorescent tags[92]. While nucleic acid sequences allow unique tagging of very large screens, they can only be detected once the screen is completed. On the other hand, fluorescent tags can be detected on the fly within a microfluidic chip but they can only offer a limited number of unique tags, hence preferred for smaller libraries requiring real-time decoding[44].

Sequencing was achieved by a slotted-vials array (SVA) platform where a tapered capillary tip was used to generate droplets via suction from slotted vials which could be rotated by a motor[93]. Later, Gielen *et al.* developed a compartment-on-demand platform[94], now productised and marketed by Dolomite Microfluidics under the brand name Mitos Dropix®. In this study, the vials were immersed in an oil bath to avoid contamination, also eliminating the need to siphon oil in between droplets. These systems can be programmed to produce any sequence of droplets from multiple samples loaded in a carousel (Fig. 1(a)). A serial sample loading (SSL) system[95] interfaces with a 96-well plate to sample the fluids in an orderly manner (Fig. 1(b)). These systems make use of robotic setup to reposition the inlet of a microfluidic chip, therefore they usually produce relatively large droplets with slow throughputs, yet they are robust, compatible and successful in the formation of a vector of droplets.

Other relevant platforms for generating droplet libraries involve creating concentration gradients by utilising controlled exchange of materials between moving plugs and stationary drops[96]. As the moving plug interacts with the stationary droplets sequentially, a concentration gradient was formed. Comparably, Niu *et al.*[97] designed a droplet dilution module using droplet microfluidics; the diluted droplets were formed through merging with a highly concentrated reservoir, diffusing briefly and then splitting from the reservoir at the other end. As the reservoir is diluted, the produced droplets had lower concentrations of the reservoir content, thereby creating a vector of droplets. Recently, the same group designed a multi-layered microfluidic device[98] which can generate a concentration gradient in one layer fed through multiple flow focusing junctions in another layer to create droplets of different concentrations (Fig. 1(c)). Furthermore, it was shown that a cross junction can be used to collect different droplets streams into a single container[99] to form the vector in an unordered manner (Fig. 1(d)). Abate *et al.*[100] designed picoinjectors to selectively add reagents into droplets and showed that droplets could be injected from three different inlets on the chip with electrical control. Another approach for generating a droplet library is through the integration of microscale chemical separation techniques such as capillary electrophoresis[101] or liquid chromatography[102,103] before the droplet formation junction. This way, the distinct bands are compartmentalised into a vector of droplets while molecular diffusion is minimised.

A vector of droplets is sufficient to create a small combinatorial library, however, when the targets grow to the order of millions, this becomes impractical. For this reason, microfluidic systems that can combine two different pools in an efficient manner are crucial for on-chip screening studies. Theberge *et al.*[99] designed an electrocoalescence fusion chip (see section 3.4) which was fed by two streams to merge and form a combinatorial library; a library of droplet emulsions formed using a cross junction (Fig. 1(d)) and another pool of chemicals pre-stored as plugs onto polytetrafluoroethylene (PTFE) tubing. Zec *et al.*[95] formed the first vector using an in-house built SSL system (Fig. 1(b)) and crossed them with droplets alternated on-demand with integrated membrane valves (see Supplementary Text †) from multiple inlets (Fig. 2(a)). Sesen *et al.*[104] demonstrated the formation of desired chemical compositions using pipette on a chip platform which makes use of surface acoustic waves to pipette droplets selectively into a side channel (Fig. 2(b)). Leung *et al.*[105] designed a microfluidic system capable of dispensing from eight different reagents into microfluidic storage chambers using integrated microvalves (Fig. 2(c)). Furthermore, Jin et al. designed a chip for droplet generation, storage, fusion and retrieval using multiple layers of PDMS membranes (Fig. 2(d)).

The formation of a combinatorial library on a microfluidic chip is essential for the evolution of screening studies. Further

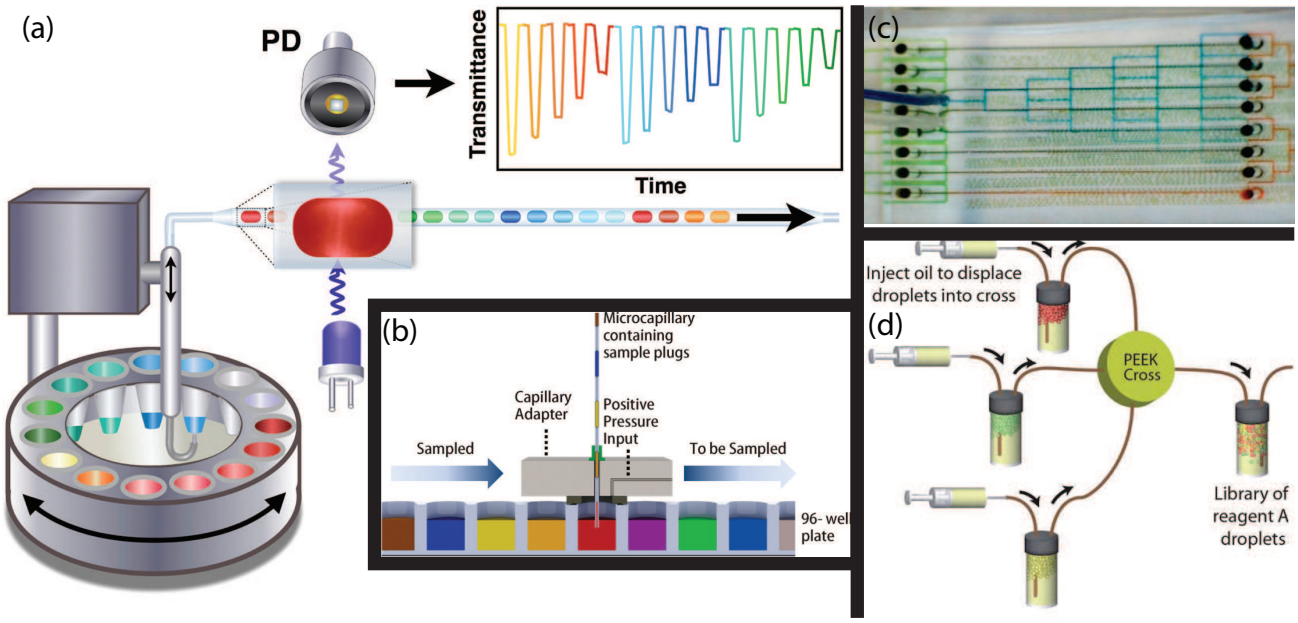

Fig. 1 (a) Compartment-on-demand platform; formation of a droplet vector by sampling from a carousel[94]. Copyright (2013) American Chemical Society. (b) Serial sample loading system is capable of sampling from a 96-well plate. Reproduced from[95] with permission of The Royal Society of Chemistry. (c) A multi-layered microfluidic chip capable of forming a concentration gradient which is later turned into droplets[98]. Copyright (2015) American Chemical Society. (d) Using a cross junction to collect different droplet samples into one container. Reproduced from[99] with permission of The Royal Society of Chemistry.

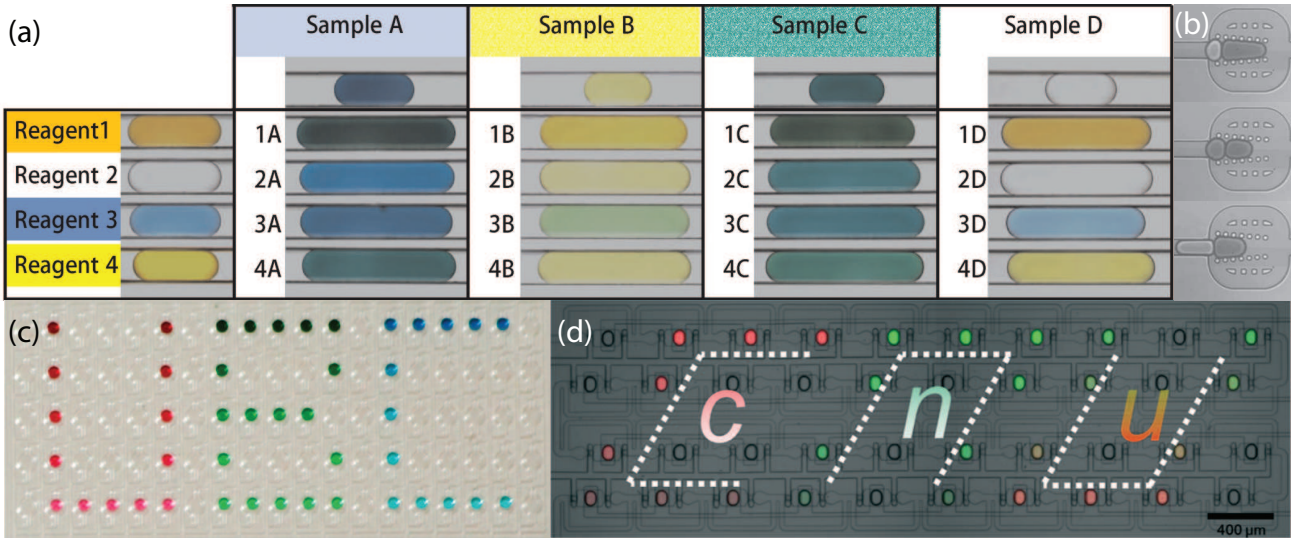

Fig. 2 Formation of a combinatorial matrix; (a) the samples are alternated via integrated membrane valves whereas the reagents are generated by an SSL system. Reproduced from[95] with permission of The Royal Society of Chemistry. (b) Alternating droplets were pipetted into a side channel with surface acoustic wave actuation to obtain various compositions[104]. (c) Addressable storage chambers for droplets generated by a network of integrated membrane valves. Reproduced from[105]. Copyright 2012 National Academy of Sciences, USA. (d) Droplets generated from four inlets can be transported to storage chambers, fused and retrieved using PDMS membranes. Reproduced from[106] with permission of The Royal Society of Chemistry.

manipulation such as incubation or mixing followed by detection could reveal the positive reaction between certain subsets of these libraries. The discussed methods exhibit unique advantages which make them suitable for certain studies; once a technique is adopted for the intended study, the droplets within the system should be controlled accurately in order to perform the required task. We will now discuss droplet control technologies with the potential to add extensive capabilities to the designed chip. Indeed, without proper droplet control technologies, dictating droplet behaviour can prove to be challenging especially at higher throughputs in closed microfluidic systems.

3 Droplet Control Technologies

The versatility of modern HTS is hard to match with microfluidic systems; micro well plates could physically be moved around using robotic machinery where upgrading or adding functionality to the process is as easy as installing new equipment within the reach of robotic arms and subsequent programming. When it comes to designing digital microfluidics for screening purposes; required droplet methods, droplet behaviour and the pre or post-analysis of the proposed system should be determined well in advance. Devices need to be designed and optimised on a per study basis because unique process flows are required for every application with multiple steps involving various droplet manipulations and post-processing capabilities. This is why there's a clear need for advanced droplet control technologies that are versatile, cross-compatible and enable automation.

Droplet manipulation can be achieved by various microchannel designs that make use of hydrodynamic forces to manipulate droplets (e.g splitting and trapping). Alternatively, droplets could be subjected to external forces such as acoustic, electric or magnetic to control droplet behaviour within microfluidic systems. Droplet behaviour can be altered by selection of chemicals, usage of surfactants or coatings on microchannel interiors; droplet microfluidics heavily depend on wall properties, surface tension, droplet-droplet interactions and surface chemistry. Moreover, identification of pre and post analysis methods such as droplet sensing, Raman spectroscopy or fluorescent light intensity measurement is of paramount importance. For example, a polymerase chain reaction (PCR) study demands rapid and accurate thermal cycling [107] whereas a single-cell study might call for droplet steering and fluorescent viability assay.

Another important aspect of HTS is its inherent selectivity; all the compounds are isolated within easily accessible micro wells. This becomes a challenge in closed droplet microfluidics where the compartments are picolitre size and moving with high throughput. Some of the developed droplet control technologies, usually active ones, offer selectivity at the cost of increased complexity whereas other methods are simpler for easy integration and high throughput while lacking selectivity. In this review, we will focus on enabling droplet manipulation and detection (pre-analysis) techniques for screening studies offering selectivity as well as those that don't and how they can all affect droplet behaviour.

3.1 Formation

The starting point for a droplet based lab-on-a-chip (LOC) device is the accurate and uniform generation of a monodisperse droplet stream. Droplet formation is usually achieved through passive techniques which take advantage of the flow field to deform the interface and promote the natural growth of interfacial instabilities [86]. There exists three main passive techniques which are widely used by researchers to generate droplets, namely, T-junctions (Fig. 3(a)), flow focusing devices (Fig. 3(b)) and step emulsification (Fig. 3(c)). Moreover, some active droplet formation techniques exist where droplet production could be triggered and the volume of the droplets produced can be altered on-demand using membrane deformation (microvalves) [106,108,109], heating [110,111], surface acoustic waves (SAWs) [112,113] or vibration [114].

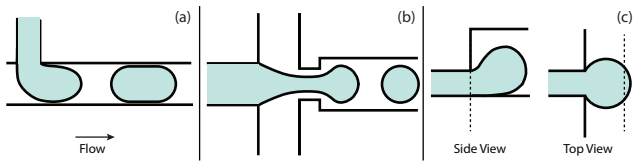

Fig. 3 Droplet generation using (a) T-junction, (b) flow focusing geometry and (c) step emulsification.

3.1.1 T-junctions

The formation of droplets in T-junctions was first observed by Thorsen *et al.* [115] who propelled two immiscible fluids through two perpendicular microchannels and examined the formation of stable droplet streams where the flows meet. T-junction droplet formation (Fig. 3(a)) has been widely used in droplet microfluidic systems since then and consequently, it was thoroughly characterised and described by researchers via numerical and experimental studies [116–119]. A number of parameters affect droplet formation in T-junctions such as capillary number (see Supplementary Text †), interfacial tension, contact angle and a few more [54].

The production of droplets using T-junction geometries can be categorised into three separate regimes; squeezing, dripping and jetting regime. When the capillary number is lower than a critical capillary number $Ca \approx 0.015$ [118,120,121], indicating that interfacial tension is significantly larger than viscous shear, the droplets grow to fill up the entire channel unobstructed by the viscous shear stress and block the continuous

phase flow until the dynamic pressure builds up in the trailing end of the droplet. This pressure build-up thins the interface as the droplet grows and finally ruptures the interface to form a droplet. Droplets formed in this way are usually not spherical and sometimes referred to as plugs meaning the droplet diameter is larger than the channel width. Plugs play a key role in screening studies because they act in a single file, therefore, sequence information is preserved in plug systems.

An important observation to note about this regime is that flow rate ratio (Q_1/Q_2) and droplet length, therefore droplet volume (V_d), are proportional to each other independent of the oil viscosity (i.e $Q_1/Q_2 \propto V_d$) as observed by Garstecki *et al.*[116]. This property significantly reduces the complexity of droplet production and allows researchers to conduct studies with different droplet volumes for better characterisation.

Furthermore, Steijn *et al.*[122] have developed a by-pass channel geometry which forces droplets to be of the same size regardless of the imposed flow rates and fluid properties. The by-pass channel is designed around the T-junction site so that the continuous phase flow is not obstructed while the droplet advances thereby preventing the rapid pressure build-up mentioned earlier. The droplet grows freely until the by-pass channel is completely blocked, after which the droplet pinches off. In this way, monodisperse droplet formation can be ensured without the need for expensive and bulky equipment because cheaper and smaller syringe pumps can incur pressure fluctuations in microfluidic devices leading to poly-disperse and irregular droplet production.

The second regime is the dripping regime where the Capillary number is high enough so that viscous shear breaks off the interface to form a droplet before the droplet grows enough to constrict the oil flow. In this regime, the flow rates and therefore the throughput is significantly higher. Moreover, the produced droplets are usually spherical and smaller than the channel width and highly monodisperse. This regime is suitable for studying high throughput screens and single-cell studies.

The jetting regime is observed when the flow rates are increased further; in this case, the dispersed phase protrudes into the main channel like a jet stream initially. Further downstream, due to high shear stress, the interface destabilises (Rayleigh-Plateau instability) and breaks off to form spherical monodisperse droplets. The jetting regime is usually preferred for particle or fibre synthesis studies[123].

3.1.2 Flow focusing & Co-flow

Flow focusing geometries (Fig. 3(b)) were first proposed by Anna *et al.*[124] and Dreyfus *et al.*[125] where the dispersed phase is pinched orthogonally by two continuous phase streams that are flowing in towards each other. On the other hand, co-flowing streams were introduced by Cramer *et al.*[126]; they exploit the instabilities arising from the continuous phase flowing from an outer ring merging with the dispersed phase flowing through an inner ring. The physics of flow focusing and co-flowing droplet generation are quite similar yet, in the literature, they are usually studied separately[82].

In a co-flowing system, the dispersed phase is injected into the continuous phase where it forms a thread. This thread quickly thins due to hydrodynamic shearing and becomes unstable. As a result, the thread decays into droplets in order to minimise the total surface area thereby reducing the free energy of the interface[86]. In a flow focusing system, the co-flowing liquids are further forced through an orifice. This stretches and thins the thread resulting in smaller droplets being produced. Similar to T-junctions, the size and frequency of the generated droplets depend on a number of parameters. Since flow focusing geometries are more complex, it has proved hard to formulate or estimate the final size and frequency using analytical approaches. Recently, Chen *et al.*[127] developed a model to predict droplet formation in flow focusing geometries working in the squeezing regime.

While flow focusing and co-flowing geometries are slightly more complicated to fabricate and operate, they offer enhanced monodispersity and higher throughputs compared to T-junction geometries. Double-emulsion studies, where single or multiple droplets are confined within bigger droplets, are usually carried out with flow focusing geometries[128,129]. It has also been argued that these geometries are preferred while working with fragile biological samples[82].

3.1.3 Step Emulsification

Microchannel step emulsification was introduced by Sugiura *et al.*[130,131] where they showed highly monodisperse droplet formation when the aqueous phase was injected through a step structure in the microchannel design, the top and side views of such a geometry is shown on Fig. 3(c). The dispersed phase first fills up a terrace opening to a deep well; this leads to an abrupt change in capillary pressure and consequent droplet break-up. Since the droplet formation is triggered by a static instability defined solely by the microchannel geometry, the produced droplet sizes are weakly or not dependent on external factors such as flow velocity or fluid properties[132,133]; a highly desirable property for droplet production in centrifugal microfluidics[134] (Fig. 4(a)). Additionally, Dangla *et al.*[132] designed an inflatable terrace and showed the formation of highly monodisperse droplets reducing microfabrication complexity as well as offering droplet volume control by adjusting inflation pressure (Fig. 4(b)). Step emulsification suffers minimally dead volumes[134] making it a powerful technique for use in applications where the droplets are further manipulated or analysed on chip such as droplet PCR on-chip[135]. Although the complexity of microfabrication is most advanced in step emulsification compared to previous techniques, as there are multiple levels of channel height, this method is scalable and therefore applicable to high-throughput monodisperse droplet

formation [133].

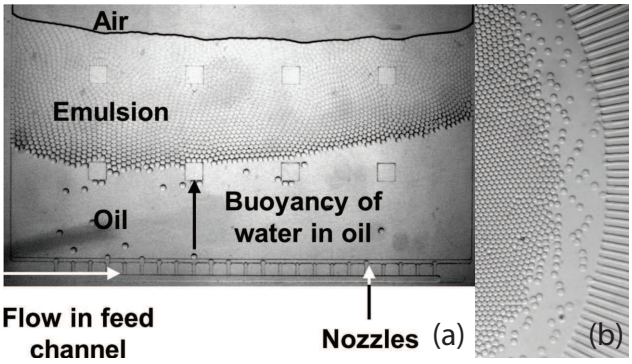

Fig. 4 (a) Droplet formation using centrifugal step emulsification. Reproduced in part from [134] - Published by The Royal Society of Chemistry. (b) Droplet formation under an inflated terrace. Reproduced from [132]. Copyright 2013 National Academy of Sciences, USA.

Droplet formation, overall, provides the 'activation energy' for starting droplet microfluidic studies; it is an extremely important first step often taken for granted. Though it also poses challenges as large numbers of identical droplets is not compatible with multiple chemicals in a range of permutations. Advanced control over droplet formation opens up a new world of possibilities such as volume control and on-demand production of pico droplets. We will discuss active droplet formation techniques next.

3.1.4 Active Droplet Formation

Despite reduced reliability and enhanced complexity, active droplet formation (also referred to as drop-on-demand) techniques form a good base for performing exhaustive assays on chips where multiple targets are to be screened in the search for the optimum recipe. The technology to produce on-demand droplets (one at a time) or from multiple inlets in order to create a combinatorial library similar to high throughput screening (HTS) poses significant challenges because microfluidic devices are planar and driven by continuous flows. Additionally, it is often necessary to finely tune the reactants with respect to their volumes for chemical screening studies, hence the reasons why this technology requires more attention. Active droplet generation designs, so far, have addressed these issues by offering droplet volume control and on/off switching capabilities. They have been successful in the production of droplets on-demand or modification of the droplet volume and frequency on the fly, sometimes both [106,108,112,113,136].

One such drop-on-demand chip makes use of a microvalve (see Supplementary Text †) implemented at a droplet forming T-junction which acts as an on/off switch for droplet production [108]. As the microvalve is relaxed for an extended period of time, resulting droplet volume increases (Fig. 5(a)). Another technique for controlling droplet formation is through applying surface acoustic waves (SAWs) (see Supplementary Text †) at the acoustic interface where droplets are formed by a flow focusing geometry [112]. This way, droplet volume and frequency could be altered on the fly. It was observed that as the SAW power is increased, droplet volume decreases whereas their formation frequency increases [112].

Collins *et al.* [113] designed a drop-on-demand system capable of producing picoliter droplets by exerting SAW induced forces on a water/oil interface which deformed into the oil stream to create droplets. Schmid and Franke, in their first work [112], directed SAWs at a flow focusing junction to modulate droplet size in real time by adjusting SAW power. In a later study, they [137] developed a microfluidic chip to govern the size of droplets forming at a T-junction with low Capillary number (Fig. 5(b)). They achieved this by inducing acoustic streaming in the continuous phase before the T-junction. Recently, Brenker *et al.* [138] showed that monodisperse droplets of 200fL could be produced on-demand using SAWs to eject droplets into the oil stream at a T-junction with a PDMS flap.

Jin *et al.* [106] integrated microvalves at multiple droplet formation sites to alternate between them programmatically. This resulted in the formation of a combinatorial matrix where droplets from four different inlets were mixed and matched with each other to generate all possible combinations (Fig. 5(d)). Alternatively, also using the approach of deformable valves, various size membranes have been integrated next to flow focusing junctions on single layer microfluidic chips allowing control over droplet volume (Fig. 5(e)) or frequency [136] (Fig. 5(f)). Choi *et al.* [109] fabricated PDMS membranes underneath two sample inlets and achieved pumping via using them as pneumatic micro-pumps in order to decrease the footprint of the microfluidic chip by eliminating the need for syringe pumps.

Enhanced control over droplet generation is essential for screening studies; precision dispensing and chemical composition control enables higher quality screens. When designing a screening study, the maximum throughput of the system should be considered. For example, a membrane system is limited by pressure regulators and solenoid valves, throughputs up to kHz [136] can be achieved with these systems. In the case of pneumatic micro-pumps [109], the throughputs were up to 8Hz but two sample inlets could readily be modulated for modifying droplet content to form a library. SAW systems are theoretically limited by the speed of sound, however, in reality, are limited by the pulse modulation capabilities of signal generators [139]. On the other hand, a Serial Sample Loading (SSL) system [95] offers multiple chemical reservoirs, therefore chemical composition control but they are operated by robotic arms significantly limiting the throughput and minimum droplet size attainable by such systems.

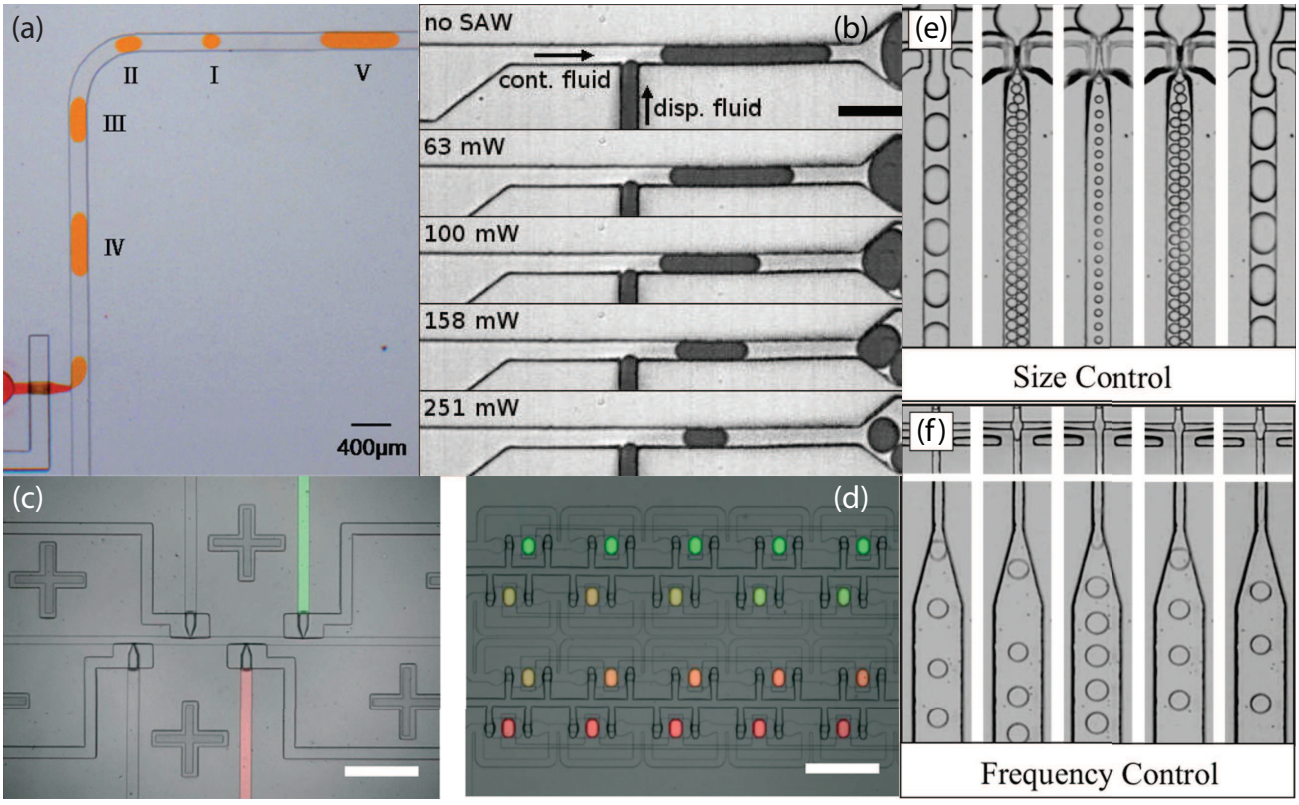

Fig. 5 (a) Droplet formation using deforming membranes. Reproduced in part from [108] with permission of The Royal Society of Chemistry. (b) On the fly droplet volume modulation using surface acoustic waves (SAWs). Reprinted with permission from [137]. Copyright 2014, AIP Publishing LLC. (c), (d) Droplet formation from different inlets using membrane deformation. Reproduced in part from [106] with permission of The Royal Society of Chemistry. (e) Droplet size and (f) frequency control using membrane deformation. Reprinted with permission from [136]. Copyright 2009, AIP Publishing LLC.

We have briefly discussed alternative methods of generating droplets for screening studies; further details on this subject could be found in a recent review by Chong *et al.*[88]. We will now investigate techniques to sense the existence of these droplets; droplet sensing adds complexity but is a key part of automation and selectivity especially when coupled with sorting.

3.2 Sensing

Sensing droplets can be an important tool when performing time-dependent studies where a droplet's exact arrival time to a specific section of the microfluidic chip is required for further manipulation such as droplet sorting. More importantly, sensing is required for selectivity and droplet automation in microfluidic systems leading to powerful, more capable LOC devices for μHTS. As the number of manipulation events increases to meet the demands of larger more complex systems, the logistics of droplet management will require precise information about the location, size, and content of droplets around the chip. In addition, quantitative studies in which the exact number of droplets passing through a section is required, sensing can generate useful information about the system. Furthermore, it is sometimes possible to determine the content or volume of a droplet during sensing; this can be very useful if there are certain physical or chemical requirements on the droplets. In cases where assaying the chemical contents within droplets are required, techniques such as mass spectrometry [140,141], Raman spectroscopy[142] and capillary electrophoresis [143] have previously been coupled with microfluidic devices; the reader is referred to specialised reviews[77,85] on this topic for detailed discussions, here we focus on the detection of droplets for further analysis. Two prominent methods of sensing droplets in closed microfluidic channels are optical and electrical detection.

Optical methods work by detecting light passing through a droplet at various wavelengths. Common detectors include charge coupled devices (CCD), photodiodes (PD) and photomultiplier tubes (PMT). An easy to implement optical detection method is a microscope-integrated high speed CCD camera with image processing where the droplets can be processed quantitatively and qualitatively by measuring their occurrence, pixel area and light refraction intensity. However, real time image processing usually requires a significant amount of computing power, therefore, throughput is usually low. Jakiela *et al.*[144] made use of a linear camera to sense droplets within a microfluidic channel. The linear camera records fewer pixels, as low as 2048, instead of the several megapixels recorded with standard CCD cameras, reducing the required computing power and so improving throughput. By analysing light intensity, the linear camera can detect the front and the back end of the droplet, thereby providing droplet velocity and volume information as well as their occurrence frequency[144] (Fig. 6(a)).

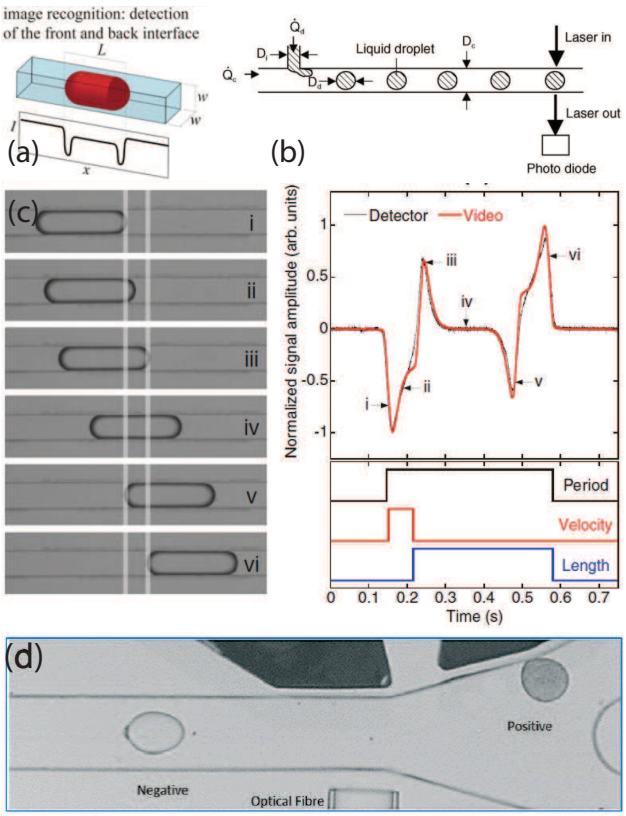

Fig. 6 (a) Using a linear camera to sense droplets. Reproduced in part from[144] with permission of The Royal Society of Chemistry. (b) Detecting droplets with a photodiode. Reprinted from[145], Copyright (2006), with permission from Elsevier. (c) A pair of photodiodes connected head to tail to sense droplets and determine their size, velocity and frequency. Reprinted from[146] with permission of Springer. (d) Sensing droplets containing bacteria using a photo-multiplier tube (PMT). Reproduced in part from[51] with permission of The Royal Society of Chemistry.

Another optical detection approach is the use of a PD for counting or timing droplets within a microfluidic system [145,146]. Nguyen *et al.*[145] integrated an optical fibre across the microfluidic channel to sense the droplets via a photodiode (Fig. 6(b)). Robert de Saint Vincent *et al.*[146] improved this method and implemented a pair of PDs connected head to tail which produces a differential signal. This signal can be interpreted at high throughputs to acquire droplet information such as size, velocity and frequency (Fig. 6(c)).

Moreover, fluorescent intensity could be measured in order to identify certain droplets based on their fluorescence. Fluorescent intensity is usually detected via a PMT[147] or APD [148]. Fluorescence activated droplet sorting (FADS) system [147] is capable of sensing cells in droplets for sorting and enrichment with throughputs up to 2kHz. Recently, a PMT was

utilised to detect the existence of bacteria in droplets to identify antibiotic-resistant colonies[51] (Fig. 6(d)). Fluorescent tagging was not used in this work, instead, light scattering from a droplet full of bacteria was compared to an empty droplet to distinguish between them at high throughputs.

Overall, CCDs can offer qualitative information about droplets at low throughputs, however, PDs and PMTs can achieve high throughputs and capture quantitative droplet information but they usually require expensive and bulky equipment such as laser beams and lenses to operate.

Electrical detection methods, on the other hand, can be implemented as electrodes on a chip where the output could be measured by microchips and analysed by computers. Two examples of electrical detection are resistive[149] and conductive sensing[150] where the electrodes are in contact with the fluid in the microchannel. The conductivity of the dispersed phase is usually much higher than that of the continuous phase so once the dispersed phase comes into contact with two open electrodes, resistance changes drastically, easily picked up by a microchip. As for resistive sensing[149]; when a conductive droplet passes over a high resistance section of the electrodes, the resistance of the sensor decreases and this can be tuned to detect droplets passing over the electrodes. Resistive and conductive methods offer superior sensitivity but require contact with the droplets in which case cross-contamination can be an issue.

To avoid such issues, capacitive sensors can be used; these are fabricated with a passivation layer to eliminate cross-contamination (Fig. 7(a)), a step, however, which comes at the expense of sensitivity. Commonly, the dielectric constant of the aqueous dispersed phase is significantly higher than its oil based counterpart, this makes capacitive sensing suitable for droplet detection[151–154]. The design of the electrodes plays an important role in the capacitive sensing of droplets. Sensing electrodes usually exhibit a capacitance of a few picofarads (pF), therefore the sensor capacitance change should be adjusted to best the microchip's sensitivity. Moreover, instead of just a pair of electrodes, multiple IDT-like electrodes can be designed to obtain information about droplet size, velocity and even content[152,154]. Kemna *et al.*[155] used an impedance measurement to sense droplets within a microfluidic chip. They showed that cell viability in low-conducting buffer and the existence of cells in droplets could be uncovered by the impedance measurement system.

Another example of electrical detection is microwave sensing[156]; a droplet passing over a spiral sensor changes its resonant frequency which can be detected by a microwave circuit that measures the reflection coefficient of the sensor (Fig. 7(b)). It was also shown that this system could be used to heat droplets up and facilitate mixing within droplets. While the rapid mixing takes place because of Marangoni stresses induced on the droplet interface[157], the heating is due to di-

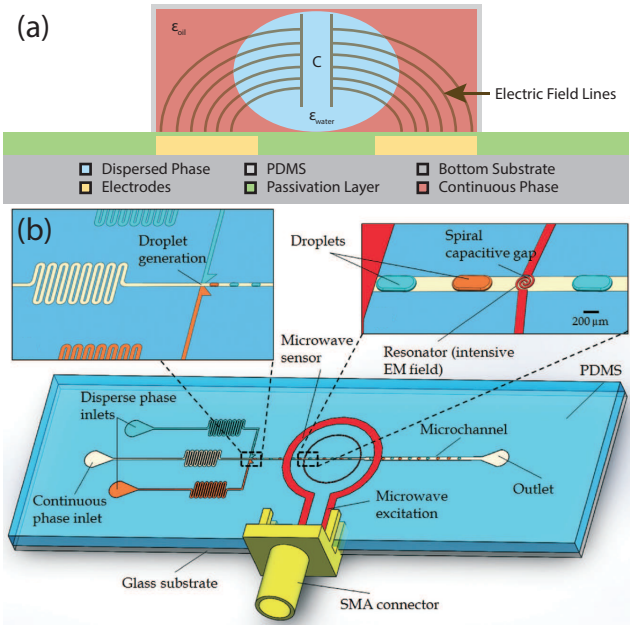

Fig. 7 (a) Cross sectional view of a representative microfluidic device demonstrating capacitive droplet sensing. Once a droplet with high permittivity passes over the capacitive electrodes, the capacitance increases. This can be picked up by a microchip to sense the droplet. (b) Microwave sensor chip showing the excitation loop and detailing droplet generation and spiral capacitive sensor sites. Reproduced in part from[156] with permission of The Royal Society of Chemistry.

electric (microwave) heating (see Supplementary Text †). Microwave heating has been used in a number of studies [158–161] to heat up and/or sense a water-based droplet and its temperature owing to water's unique properties (loss tangent of 0.157 at 3 GHz) that allow it to absorb microwave energy quite efficiently especially at frequencies between 3 and 20 GHz. This is exactly the same technology used in commercial microwave ovens.

A sensing component, in its simplest form, registers spatiotemporal information for every droplet. More advanced sensing systems can determine droplet volume, velocity, content and even temperature. This valuable information can be used for further manipulations depending on specific chip requirements. Unwanted droplets could exist in the system such as with single-cell encapsulation in droplets where cells usually are distributed into droplets according to Poisson distribution. In such cases; in order to get rid of the unwanted droplets or conversely to collect desired droplets, sorting at junctions could be implemented. Different techniques to sort droplets at junctions will be discussed in the upcoming section.

3.3 Sorting

The ability to sort the generated droplets on-demand is crucial in the design of lab-on-a-chip (LOC) devices for screening studies. Some droplet microfluidics studies require droplets to be sorted into different outlets thereby getting rid of unwanted droplets or collecting wanted droplets into one specific channel; a great step towards automating droplets for μHTS. More often than not, the distinction between wanted and unwanted droplets is identified by droplet sensing systems or labelling discussed in the previous sections.

A common method to achieve droplet sorting starts with biasing one of the two outlets so that the droplets automatically steer into the low resistance channel in the absence of external actuation. Once a droplet is identified as unwanted or desired, however, the information can be used to trigger an actuation mechanism which would then work to steer that droplet to the unbiased higher resistance channel. Although biasing is a convenient and reliable method for steering droplets, the outlet resistances have to be carefully maintained in order for the system to work. Moreover, cross-compatibility and further manipulation after sorting can be hindered due to biasing.

Microfluidic droplet sorting devices have been designed with mechanical actuation [162] but they were prone to slow response times due to the large relaxation times of pumping systems [163]. One of the most promising droplet sorting technique utilises dielectrophoresis [147,164,165] (Fig. 8(a),(b)) where the droplets are attracted into the outlet channels by DEP forces. This method depends on the gradient of the electric field, therefore, high voltage (several kV's) is needed to apply sufficient forces with these applications [166].

Intense electric fields can be used to actuate droplets in microfluidic channels. Electric fields can easily be generated within lab-on-a-chip (LOC) devices by depositing electrodes on the substrate. Either direct current (DC) or alternating current (AC) can be applied to generate localised electric fields. Two of the commonly used droplet manipulation techniques utilising electric fields are electrophoresis and dielectrophoresis (DEP) (see Supplementary Text †).

Dielectrophoretic droplet sorting was implemented in a droplet based HTS chip for directed evolution [165]. The waste channel has lower resistance (i.e biased) in this work and the droplets, detected by a fluorescent sensor, are attracted towards the keep outlet (Fig. 8(a)) at rates exceeding 2kHz. In a recent study by Liu *et al.* [51], DEP was used to sort droplets for HTS of antibiotic-resistant bacteria using light scattering data to identify proliferating cells. These works are great examples demonstrating the capabilities enabled by μHTS.

Dielectrophoretic droplet sorting was first proposed by Ahn *et al.* [164] where they showed successful sorting at a Y-junction without biasing (Fig. 8(b). Pre-charged droplets can be attracted by an electric field for sorting [166,167] as well (Fig. 8(c)); this reduces the high voltage requirement for steering droplets, however, charging droplets requires an additional splitting step and can sometimes be harmful to the content of the droplets. Dielectrophoretic droplet sorting was first proposed by Ahn *et al.* [164] where they showed successful sorting at a Y-junction without biasing (Fig. 8(b). Pre-charged droplets can be attracted by an electric field for sorting [166,167] as well (Fig. 8(c)); this reduces the high voltage requirement for steering droplets, however, charging droplets requires an additional splitting step and can sometimes be harmful to the content of the droplets.

Droplets can be labelled with magnetic beads or ferrofluid can be used as the dispersed phase [168]; this enables the use of magnetic sorting [169]. Such droplets respond to magnetic fields generated inside microfluidic devices due to their magnetic content. Whilst high sorting rates can be achieved, magnetic labelling can be undesirable especially when working with delicate biological samples.

Additionally, droplets could be sorted with surface acoustic waves (SAWs) [163] (Fig. 8(d)). In this case, Franke *et al.* [163] made use of a biased Y-junction design where the droplets preferentially followed the upper channel (low resistance) in the absence of SAWs. When the IDTs are excited, however, SAWs couple into the continuous medium and induce acoustic streaming. This streaming agitates the continuous medium which in turn displaces droplets laterally and forces them to be steered into the high resistance outlet channel. More recently, this SAW technique was used to design a fluorescence activated droplet sorting system with three outlets exhibiting throughputs up to 3kHz [170]. Multiple PDMS posts were used for acoustic energy coupling allowing inexpensive

PDMS chips to be disposed while costly lithium niobate substrates can be recycled[170]. Li *et al.*[171] designed a five outlet channel and used standing surface acoustic waves to guide droplets into desired outlets with throughputs up to 222Hz limited by electrical signal switching capability.

Moreover, SAWs have been used to steer plugs completely or split them unevenly at a specially designed Y-junction (Fig. 9(a),(b))[172]. SAWs have been directed to the interface of the plugs to displace them into one or the other outlet which were not biased during the study[172]. The system demonstrated here can sort larger plugs into any of the outlets (Fig. 9(a),(b)) without loss of valuable sequence information. Moreover, it offers control of even or uneven splitting of the plug at the Y-junction in a programmable manner.

SAWs are not the only way of using vibration to govern droplet behaviour, Leibacher *et al.*[173] made use of bulk acoustic wave (BAW) acoustophoresis to handle droplets in a silicon chip. By forming and controlling the ultrasonic standing wave in the bulk fluid, they were able to sort droplets (Fig. 9(c)), move them across mediums for washing and merge them. Recently, Phan *et al.*[174] designed a microfluidic chip with a membrane whose resonant frequencies were excited by a piezoelectric transducer. It was shown that droplets flowing in a continuous stream with a surfactant could be moved to another oil stream that was surfactant free (Fig. 9(d)). This way, spontaneous merging between selected droplets could be achieved further downstream.

Evidenced by all of these studies, biasing is a common method used in droplet sorting; electric fields and SAWs are two major actuation mechanisms for this purpose. Additionally, BAWs present a powerful and easy to integrate alternative droplet handling method. Further discussion on droplet sorting techniques could be found in a recent review by Xi *et al.*[89]. Droplet sorting and merging are two essential tools that often go hand-in-hand, therefore, droplet merging techniques will be discussed in full in the next section.

3.4 Merging

Selective droplet coalescence using microfluidic systems Cite this: Lab Chip, 2012, 12, 1800 Linas Mazutis*abc and Andrew D. Griffiths

Chemical and biological analysis commonly needs coalescence (fusion) of different liquids (e.g., samples and reagents) to complete the reactions[175]. Reactions in droplets can be used for a number of applications, including the formation of particles, chemical synthesis, kinetics studies, or for the synthesis of biomolecules[81]. Droplet microfluidic systems offer the advantage of isolated droplets which could be merged to serve as compartments in which to study fast organic reactions[176]. Moreover, coalescence allows switching back to bulk methods; for instance, after isolating rare cells from a complex sample by using droplet microfluidics, desirable samples can be rejoined for further analysis easily performed by conventional techniques. This is why another essential component of a potential versatile LOC device for screening studies would be the capability of merging consecutive or selected droplets so that reactions in droplets could be studied.

There are multiple factors that affect droplet fusion such as wall wetting properties, microchannel geometry, capillary number, surfactants, liquid viscosities and impact velocity but they have not yet been characterised thoroughly[177]. The most commonly used model to predict droplet coalescence is the film drainage model which will be explained with a brief overview.

3.4.1 Without Surfactants

Aqueous droplets in oil streams free of surfactants merge spontaneously upon contact or within close proximity due to film drainage effects (Fig. 10 (a)). There exists a film of continuous medium between two adjacent droplets which prevents coalescence and the time it takes for this film to reduce its thickness by half is given as[178]:

$$t_{drainage} = 40r\sqrt{\frac{\mu_c}{\gamma u}} \quad (1)$$

where r is droplet radius, μ_c is the viscosity of the continuous medium, γ denotes the interfacial tension between the liquids and u is the constant approach velocity. As soon as the liquid film thins out, intermolecular forces come into play and rupture the interface, allowing merging to take place[177]. For example, we described a microfluidic droplet merging system without the use of surfactants[179]; when the parameters from this study are substituted into equation 1, $t_{drainage}$ can be calculated as 120 ms. This exemplifies how quickly fusion occurs in the absence of surfactants.

Furthermore, it has been shown that there exists a critical capillary number (see Supplementary Text†), $Ca_c \approx 10^{-2}$, that determines the threshold for droplet merging to succeed [177,180]. If the capillary number is less than this critical value (i.e $Ca < Ca_c$), then droplet coalescence is more likely to occur.

3.4.2 With Surfactants

More often than not, surfactants are added to the continuous phase to carry out microfluidic studies. The addition of surfactants finds widespread usage by researchers because it reduces interfacial tension for easy droplet generation and transport, prolongs stability in a closely packed droplet formation and prevents cross-contamination so droplets can be used as individual microreactors. The reader is referred to Baret's comprehensive review on surfactants used in droplet microfluidics [181].

The downside of adding surfactants is that it undermines the spontaneity of droplet coalescence due to two main phenom-

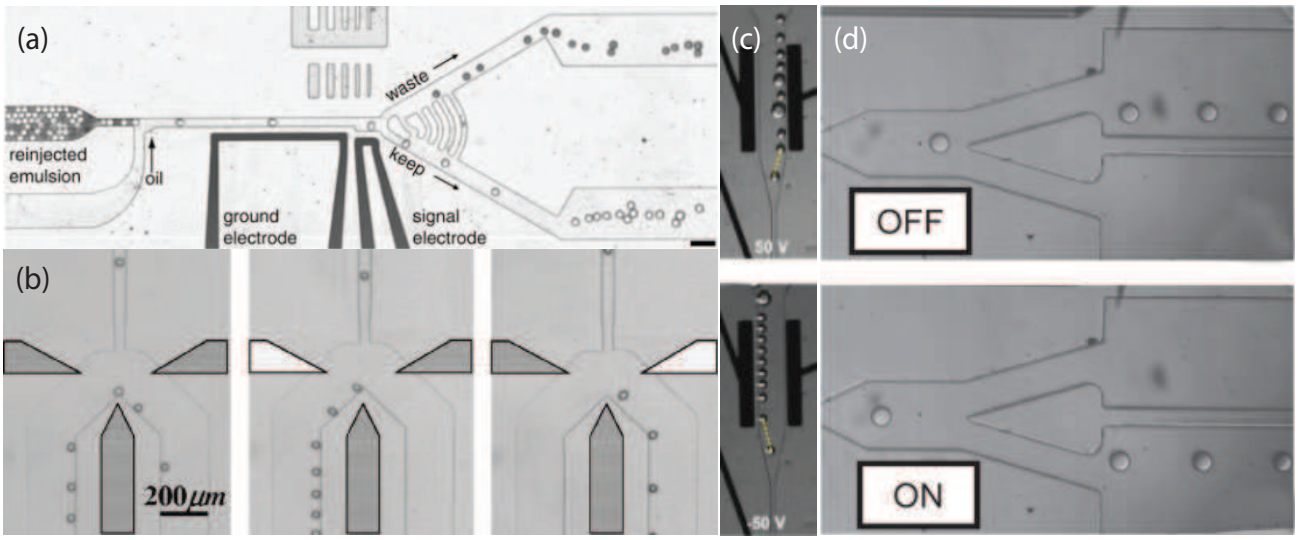

Fig. 8 (a) Dielectrophoretic sorting of droplets. Reproduced from [165]. Copyright 2010 National Academy of Sciences, USA. (b) Microfluidic sorting of droplets utilising dielectrophoresis. Reprinted with permission from [164]. Copyright 2006, AIP Publishing LLC. (c) Sorting of pre-charged droplets subjected to transverse electric field. Reproduced in part from [166] with permission of The Royal Society of Chemistry. (d) Sorting of droplets with surface acoustic waves. Reproduced in part from [163] with permission of The Royal Society of Chemistry.

ena; surfactant repulsion and Marangoni effect. Surfactants coat the interface of the droplets and they strongly repel each other, in this way the liquid film thickness does not thin out and the droplets maintain stability. Moreover, Marangoni effect takes place which creates a counter-flow in the liquid film thereby slowing down the liquid film drainage process. This effect is shown in Fig. 10(b) where the red arrows indicate the direction of Marangoni flow.

Marangoni flow occurs due to discontinuities in the surface tension of the interface where a higher surface tension will pull its surrounding liquid more strongly compared to a lower value. Since the surfactant is responsible for altering the surface tension of the droplets, the surfactant concentration near the droplet interface plays an important role in modifying the local surface tension of individual droplets. The immediate surfactant concentration at the liquid film interface can become uneven due to factors such as flow and molecular diffusion [177] thereby leading to discrepancies in the surface tension around the droplet which results in Marangoni flows that delay the film drainage and consequently increase droplet stability.

Since coalescence of microfluidic droplets is not usually spontaneous, researchers have come up with methods to ensure that fusion takes place; Feng *et al.* [177] extensively reviews these techniques. Two main methods find widespread usage for microfluidic droplet merging, namely, active electrocoalescence [167,182–184] (Fig. 11(a),(b)) and passive hydrodynamic methods [185,186] (Fig. 11(c),(d)).

It's widely known that if a droplet-droplet interface is subjected to intense electric field, the interface ruptures and droplets fuse even in the presence of surfactants. This is termed electrocoalescence. This requires the conductivity and permeability between two immiscible fluids to be different which is usually the case [87,190–193]. The reader is referred to Eow and Ghadiri's paper for detailed physical discussions on electrocoalescence [191].

Passive hydrodynamic merging of droplets, however, relies on high impact velocity of droplets and prolonged adjacency achieved through clever microchannel geometry designs and requires no external actuation. Generally, a speed bump is introduced further downstream to the formed train of droplets. When a droplet flows through the speed bump zone, its velocity decreases either due to designed physical restrictions [185] (Fig. 11(c)) or due to an expansion in the channel [186,194,195]. The trailing droplet comes in fast and then fusion takes place between the two droplets or more. Recently, Akartuna *et al.* [196] designed a passive droplet merging system by introducing a secondary stream targeted at the interface of paired droplets stabilised by a surfactant. The secondary stream included a poor solvent for the surfactant leading to cohesion and rupture of the droplet interfaces (Fig. 11(b)). Passive merging techniques offer reliability and ease of integration, however, they lack selectivity.

More recently, droplet merging has been achieved by the aid of membrane deformation which can induce pressure bursts to induce merging [187] (Fig. 11(d)) or trap multiple droplets in storage chambers [106,188] (Fig. 11(e)). Furthermore, Tullis *et al.* [189] managed to trap multiple droplets in surface energy wells and flushed the system with oil without surfactant to fa-

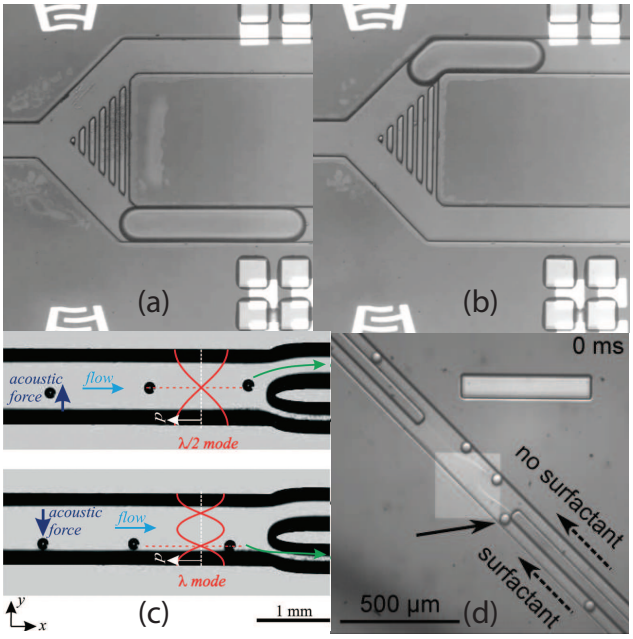

Fig. 9 Microfluidic plug steering using surface acoustic waves (SAWs). (a) The plug can be completely steered into lower channel if top IDTs are actuated [172]. (b) The plug can be completely steered into upper channel if bottom IDTs are actuated [172]. (c) Droplet sorting using BAW acoustophoresis; the half wavelength (top) and the full wavelength modes determine the droplet trajectory. Reproduced in part from [173] with permission of The Royal Society of Chemistry. (d) Droplets are steered from an oil phase containing a surfactant to one without using vibrating membrane [174]. Copyright (2016) American Chemical Society.

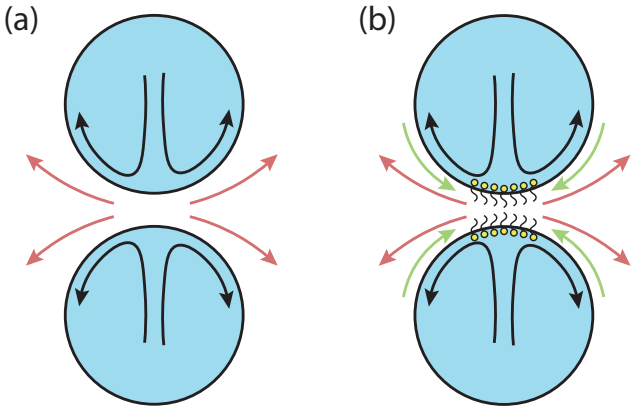

Fig. 10 (a) Film drainage (red arrows) schematic with the absence of surfactant and (b) with the surfactant where Marangoni stress (green arrows) counteracts film drainage.

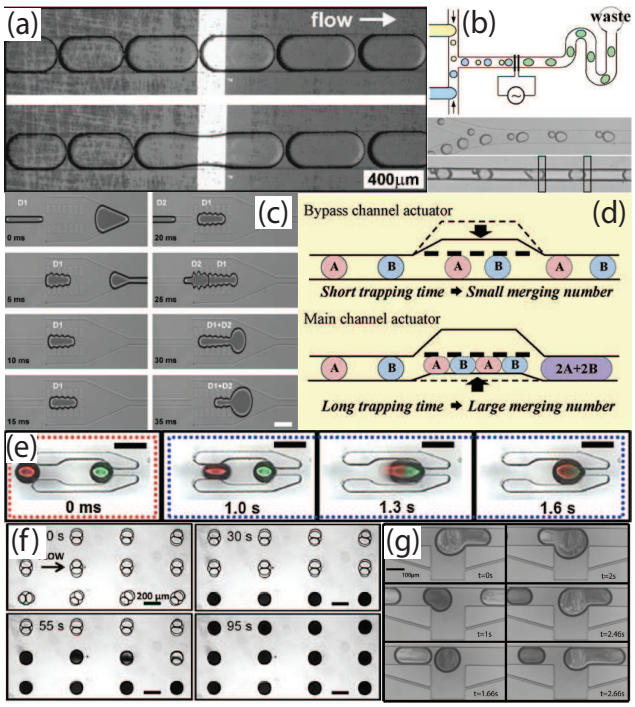

Fig. 11 (a) Droplet merging with electrocoalescence. Reprinted with permission from [183]. Copyright 2006, AIP Publishing LLC. (b) Electrocoalescence of synchronised droplets. Reprinted with permission from [182]. Copyright 2006, AIP Publishing LLC. (c) Pillar droplet merging where the droplet is trapped within pillars until a second one comes and physically merges with the trapped droplet. Reproduced in part from [185] with permission of The Royal Society of Chemistry. (d) Droplet merging assisted by membrane deformation. Reproduced in part from [187] with permission of The Royal Society of Chemistry. (e) Droplet trapping and merging within microfluidic traps using pressure bursts induced by deforming membranes. Reprinted from [188] with permission of Springer. (f) Droplet trapping into surface energy wells followed by flushing with surfactant-free carrier fluid leads to coalescence of trapped droplets. Reproduced in part from [189] with permission of The Royal Society of Chemistry. (g) Droplet merging using surface acoustic waves where the droplets are trapped within the acoustic field until the next droplet comes and merges with the trapped one. Reproduced in part from [179] with permission of The Royal Society of Chemistry.

cilitate fusion (Fig. 11(f)). In both of these recent studies, since the droplets are already trapped prior to fusion, fast reaction kinetics studies could be performed with high accuracy because the merging could be controlled.

Droplet merging was also achieved by acoustically trapping incoming droplets within a chamber until successive droplets coalesced with the trapped one[179] (Fig. 11(g)). In this work, surface acoustic waves (SAWs) were directed to the droplets in the micro expansion chamber which lead to acoustic-tweezers-type trapping of the droplets in the high pressure zone. As consecutive droplets reached the chamber and collided into the trapped droplet, fusion took place. Once the droplet in the chamber reached a certain size limit, acoustic forces were overcome by drag forces and the merged droplets exited the trapping chamber. This technique allows on-demand, controlled merging of consecutive droplets where the sequential formation of various droplets could be utilised to carry out a combinatorial droplet library study, however, the acoustic impedance of the liquids play an important role for this type of trapping to work[179].

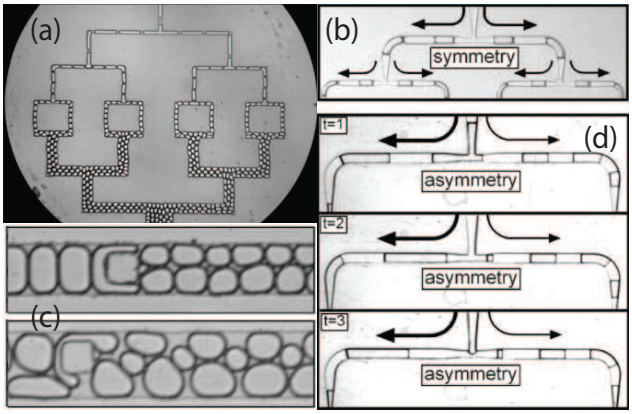

Fig. 12 (a) Symmetric droplet splitting. Reprinted figure with permission from[199], Copyright (2004) by the American Physical Society. (b) Symmetric droplet splitting. Reproduced in part from [198] with permission of The Royal Society of Chemistry. (c) Asymmetric droplet splitting. Reprinted figure with permission from[199], Copyright (2004) by the American Physical Society. (d) Asymmetric droplet splitting. Reproduced in part from[198] with permission of The Royal Society of Chemistry.

3.5 Splitting

In the context of droplet generation, it was previously mentioned that different chemicals can be introduced into a chip by robotic setup utilising a movable inlet. Due to the speed of such movement, the resulting droplets produced tend to be large in nature. As such as a counterpart to the previous section on controlled droplet merging, a very promising tool is the controlled splitting or fission of droplets.

Droplet splitting is a versatile method that helps to reduce the droplet volume[175], to control the concentration of chemicals inside the droplets[197] and to produce arrays of droplets for high-throughput screening applications[198]. Since each droplet can serve as a vessel for reagents, by splitting the single droplet into two or more droplets, the experimental capacity can easily be scaled up[81].

Droplet splitting can be achieved without external components or powered actuation: single or multiple bifurcating junctions. As a droplet is flowing through a bifurcating junction, it is affected by the shear forces occurring due to channel design. If the interfacial tension could be overcome by the shear forces, droplets split into two or more daughter droplets. The symmetry of the junction could be modified to adjust the relative sizes of the daughter droplets. A perfectly symmetric junction would lead to the break-up of a droplet into two equal sized droplets[198–200] (Fig. 12(a),(b)), whereas with an asymmetric junction, the droplet will be divided into two unequal daughter droplets[201] (Fig. 12(c),(d)). It has also been shown that two daughter droplets of different concentrations could be obtained by an asymmetric bifurcation junction[197].

In complex screening studies involving many reagents, the ability to actively control and induce splitting is often desired. At the expense of added complexity, droplet splitting can be achieved by utilising surface acoustic waves (SAWs) offering advanced control over this powerful method[104,172,202]. In one example, SAWs are directed at the oil/water interface whilst approaching a Y-junction (Fig. 13(a)) to achieve uneven plug splitting. When the travelling SAWs (TSAWs) act on the interface, it deforms away from the TSAWs into the desired outlet channel. Depending on the power of the applied TSAWs, the extent of splitting can be controlled[172]. Another design makes use of a by-pass loop integrated to the main microfluidic channel; droplets passing this junction does not split in the absence of SAWs[104]. Once the SAWs are generated, they propel the continuous medium in the upper section of the by-pass loop which leads to a strong suction effect at the by-pass entrance junction when a droplet is passing through. Depending on the duration of the applied SAWs, a portion of the main droplet can be pipetted into the by-pass channel (Fig. 13(b)). In addition, a capacitive droplet sensor is integrated upstream of the junction to accurately time the application of the SAWs enabling automation. This automated pipette on a chip system also allows the user to select which droplets should be split by how much into the by-pass channel where they can be further manipulated (i.e merged or trapped)[104]. Finally, Jung *et al.*[202] targeted SAWs directly on a droplet to thin its interface leading to rupturing and on-demand splitting (Fig. 13(c)); by controlling the acting region, droplets could be split into desired sizes.

Droplet splitting technology is being revisited as evidenced

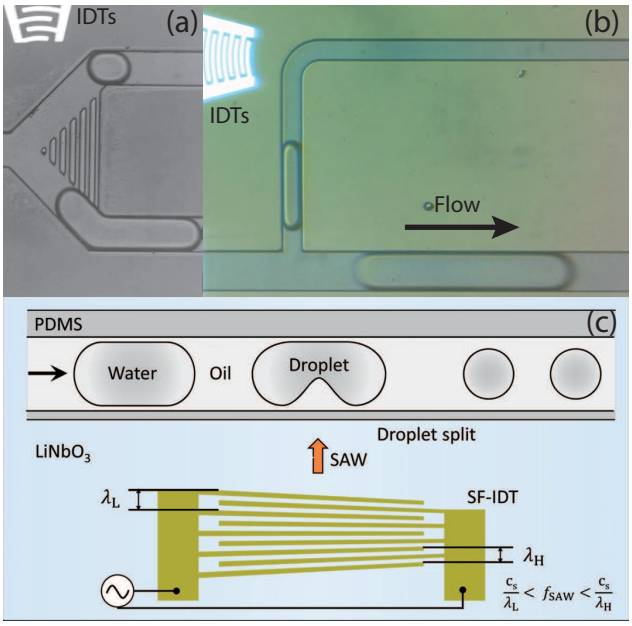

Fig. 13 (a) SAWs generated by the IDTs deform and push the plug interface into the bottom channel at a specially designed Y-junction leading to the asymmetric splitting of the plug depending on the intensity of applied acoustic energy [172]. (b) SAWs directed at a by-pass channel propel the continuous fluid to induce suction of a plug into the by-pass channel controlled by the duration of applied SAWs [104]. (c) SAW induced droplet splitting by shearing the interface until it ruptures as it is passing IDTs. Reproduced in part from [202] with permission of The Royal Society of Chemistry.

by the recent research efforts on the subject [104,172,202]. Arguably, fission was regarded as a straightforward and reproducible passive droplet manipulation technique but recent advancements, especially the emergence of drop-on-demand and serial sample loading technologies that offer droplet sequencing, are demanding for advanced droplet splitting technologies that offer better control, selectivity and enable automation. A similar argument could be raised for droplet trapping, discussed in the upcoming section.

3.6 Trapping

Given the fast nature of high throughput screening (HTS) applications, it is not easy to track a single droplet to observe the reaction occurring within. A better approach is to trap a droplet, observe while the droplet is immobile and then release the droplet for further manipulation. However, given that microdroplets of pL size are highly mobile and not rigid, it is quite hard to trap them. Researchers have developed various novel methods to overcome this problem.

One method is to design appropriate micro parking spaces for droplets within the microfluidic device [101,203–205] (Fig. 14(a),(b)). When the droplets arrive at the parking spaces, they passively get trapped usually due to higher interfacial tension imposed by the small channel geometry. Abbyad *et al.* [206] demonstrated successful trapping and releasing of droplets in surface energy wells (Fig. 14(c)). Surface energy wells can be achieved by microfabricating small holes or railways at the roof of a microfluidic device [189,206,207]. When a droplet encounters a surface energy well, it's local surface tension increases due to small channel dimensions. The higher surface tension in the energy well counteracts the fluid drag on the droplet; in this way, the droplet stays trapped in the desired area.

These passive designs might lead to the loss of sequence information which is crucial to high throughput screening applications like drug screening [99], therefore, research on active and controlled droplet trapping has gained influence over the last few years. Wang *et al.* [208,209] managed to selectively trap droplets into micro chambers by utilising dielectrophoretic (DEP) forces (Fig. 14(d)). The droplets were subjected to DEP forces when passing near the electrodes, therefore they were polarised and pushed into micro chambers where further observation could take place. Leung *et al.* [105] used a network of pneumatic actuated valves to control flow in and out of multiple droplet storage chambers (Fig. 14(e)). de Ruiter *et al.* designed electrostatic potential wells to guide and hold droplets in place [210]; they were also able to split droplets by applying higher voltages. Jin *et al.* [106] reported a static droplet array, controlled by membrane deformation where they demonstrated mixing capability for trapped droplets via membrane fluctuation (Fig. 14(f)). Recently, Jung *et al.* [211]

designed three droplet traps where they demonstrated the programmable capture and release of droplets into these traps by utilising slanted IDTs (Fig. 14(g)). To trap a droplet, they excited a frequency right after the trap so that the flow is blocked in that direction, forcing the droplet to enter the microfluidic trap. To release a droplet, they actuated a frequency that generates SAWs targeted directly under the trapped droplet pushing the droplet out of the trap due to acoustic radiation forces.

To summarise, passive droplet trapping techniques have evolved significantly offering added capability such as droplet guiding and controlled fusion for fast kinetics studies. At the same time, active and controllable droplet trapping technologies have recently emerged, especially using membrane valves to address individual compartments where different droplets could be merged and studied. The latter promises significant advancements towards the realisation of μHTS, especially in the formation of a combinatorial library.

4 Integrated Systems

In this section, we will look at how the previously described techniques are being translated into research in academia and products in industry. This will provide an insight into how these ideas are being implemented within the context of specialised research. Furthermore, it will give an improved understanding of the requirements for the individual capabilities.

We have briefly touched upon end-user products offered by companies such as 10x Genomics, Bio-Rad and Dolomite Microfluidics in the introduction section. Users of these droplet microfluidic products are already reporting significant reductions in reagent usage and processing times[64,65] rendering these products highly desirable in the market. Firstly, they interface with chemicals provided by the user, usually from well plates, a big engineering challenge in itself. They are capable of contamination-free sampling from these reservoirs to generate droplets in a high throughput manner. The aqueous phase can be complex, fed from multiple inlets joining before a flow focusing junction, including various samples such as reagents, molecular probes, cells and hydrogel beads with unique molecular identifiers[212]. Finally, the droplets are collected into vials or detected via fluorescent excitation. The implementation of droplet generation and sensing techniques are indicative of room for development in the industry; as soon as the robustness of other droplet control technologies is established, we expect they'll be implemented in products for non-specialist users.

Academia, on the other hand, has been using these technologies extensively, designing integrated systems for targeted studies. We have carefully selected 8 recent studies that integrate multiple droplet control technologies to carry out a specialised assay decreasing the costs and the time required significantly. The workflows reported in these studies are tabulated as flow charts in figure 15 sorted by publication date. The rounded rectangle denotes a chemical whereas the sharp rectangles are for processes. Dashed orange boxes indicate off-chip operations and solid blue is used for on-chip techniques.

Fallah-Araghi *et al.*[213] designed a procedure for gene enrichment using a cell free coupled *in vitro* transcription translation (IVTT) system. In this study, single DNA templates are encapsulated in droplets along with PCR mixture and collected off-chip for thermocycling amplification. The droplets containing many copies of the same gene are reinjected into a second chip where they are paired and merged with IVTT mixture using electrocoalescence. They are then incubated off-chip for transcription and translation before reinjection into a third chip for fluorescent detection followed by active emulsion breaking using a secondary aqueous stream and electric field (Fig. 15(a)).

Debs *et al.*[214] presented a method for functional screening of hybridoma cells starting with cell encapsulation in droplets along with recombinant enzymes in the first chip. These droplets are then collected for off-chip, 6h long incubation to increase antibody concentration. Reinjected droplets are passively merged on a second chip with smaller droplets containing substrates and the oil drained from around them for on-chip incubation. After incubation, the droplets are spaced again for fluorescence activated droplet sorting (FADS) (Fig. 15(b)). By extracting droplets with low fluorescence intensities, cells expressing the inhibitory antibody can be collected from the mixed population.

Sjostrom *et al.*[215] designed an on-chip incubator with multiple time-resolved observation points for studying enzyme kinetics and inhibition. Enzymes are initially mixed with different concentrations of inhibitors tagged by unique fluorescent tags for droplet production. An electrode coupled pico-injector was integrated on chip allowing the injection of a buffer+substrate solution to the formed droplets which are then incubated along delay lines for multiple observations at various time intervals for studying inhibitory characteristics (Fig. 15(c)). The concentration through the picoinjector can be regulated on-the-fly by changing relative input flow rates.

Eastburn *et al.* developed a workflow (Fig. 15(d)) to prevent reverse-transcriptase PCR (RT-PCR) inhibition due to cell lysate[216]. Microdroplet encapsulation of cells and lysis buffer was carried out in a microfluidic chip followed by off-chip incubation to activate proteinase K digestion for 15 minutes before increasing temperature for denaturation. The resultant cell lysate is then reinjected and electro-actively merged with a larger water droplet for dilution. The diluted drops are split at a Y-junction before RT-PCR mix is picoinjected into them with the aid of another electric field. Finally, the droplets are collected and heat cycled for off-chip or on-chip fluorescent detection (Fig. 15(d)).

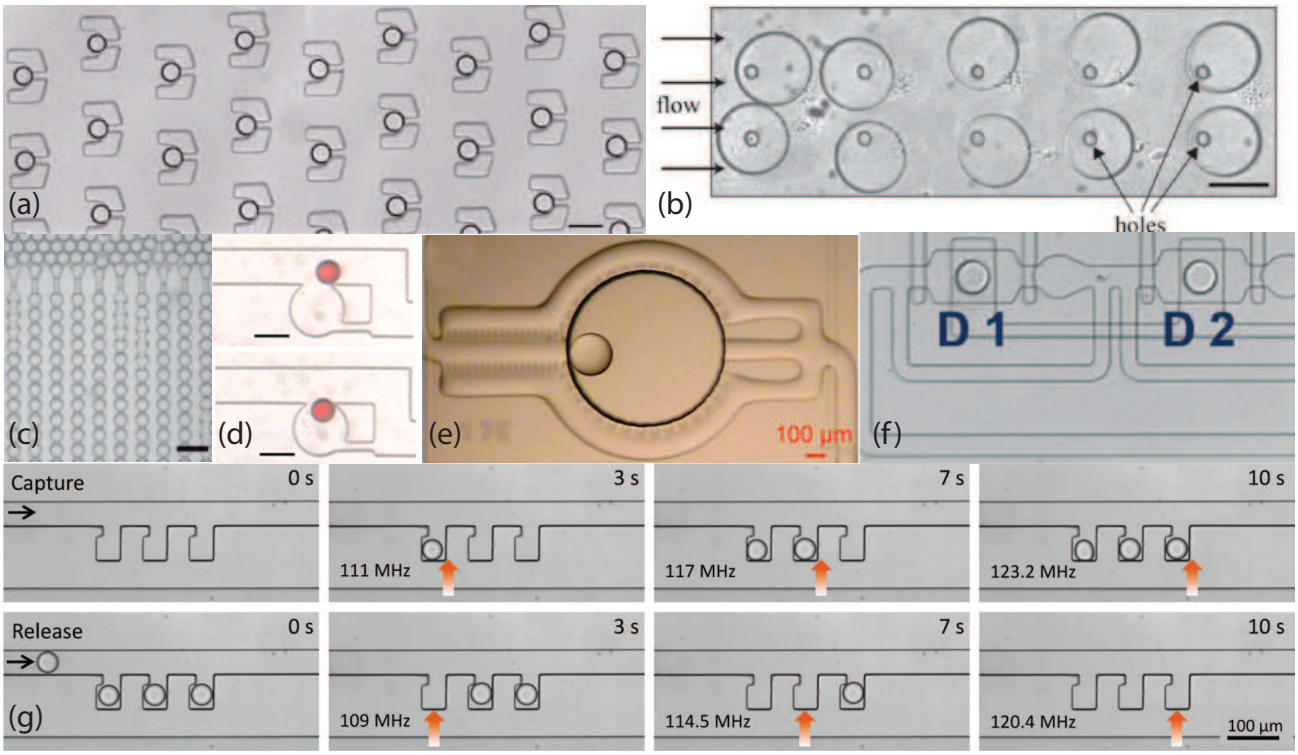

Fig. 14 (a) Static droplet traps. Reproduced in part from [203] with permission of The Royal Society of Chemistry. (b) Droplet trapping at micro parking spaces. Reproduced in part from [204] with permission of The Royal Society of Chemistry. (c) Droplet trapping at surface energy wells. Reproduced in part from [206] with permission of The Royal Society of Chemistry. (d) Droplet trapping in micro chambers with dielectrophoresis. Reproduced in part from [208] with permission of The Royal Society of Chemistry. (e) Droplet storage chambers addressed by a network of pneumatic valves. Reproduced from [105]. Copyright 2012 National Academy of Sciences, USA. (f) Droplet trapping array allowing mixing of trapped droplets by fluctuating membrane. Reproduced in part from [106] with permission of The Royal Society of Chemistry. (g) Droplet trapping and release demonstrated with three droplet traps using slanted IDTs to generate SAWs. Reproduced in part from [211] with permission of The Royal Society of Chemistry.

Recently, Lim *et al.* used droplet microfluidics to capture rare bacteria[217]. In this work, heterogeneous population of bacteria with and without mutations were encapsulated in droplets along with PCR reagents and TaqMan probes targeted at specific genes. The emulsion was then collected for TaqMan PCR amplification via thermocycling; targeted genes are rendered fluorescent by using this technique. Upon reinjection, the droplets were spaced and sorted by FADS for enrichment and isolation. Finally, the sorted droplets were collected for off-chip emulsion breaking and subsequent sequencing (Fig. 15(e)).

Huang *et al.*[218], devised a chip based approach to improve recombinant protein production of a yeast strain, subjected them to UV mutagenesis and encapsulated them in droplets for off-chip incubation. Upon reinjection into a second microfluidic chip, proliferating strains were identified by FADS and collected for DNA sequencing (Fig. 15(f)). By combining high throughput microfluidic techniques with whole genome sequencing, desirable mutations are enriched for identification.

Unique droplet barcoding by nucleic acid sequences has recently been demonstrated for single-cell RNA sequencing (scRNA-seq)[219]. In the work presented by Lan *et al.*[220], a different barcoding approach has been implemented where single DNA molecules are first encapsulated in droplets for thermocycling amplification. The amplified targets are sampled by droplet splitting to reduce volume and merged with transposase for offline incubation to randomly fragment the DNA in the droplets. The fragmented DNA droplets, barcoded droplets and droplets containing PCR mix are merged as a trio by electrocoalescence which is split again and collected for thermocycling and sequencing (Fig. 15(g)). Barcodes are attached to the fragmented DNA by overlap-extension PCR.

Pekin and Taly recently discussed their method of screening for KRAS mutations[221] in detail[222]. Since there are seven common mutations in the KRAS gene, they used a seven inlet flow focusing chip to encapsulate probes for these mutations along with different concentrations of fluorescent dye for unique tagging. The mixed pool is then reinjected and paired with droplets containing the target DNA as well as TaqMan reagents. The paired droplets are passively merged and collected for thermocycling. Finally, these droplets are reinjected for on-chip fluorescent detection to identify mutations the gene (Fig. 15(h)).

The presented studies and products clearly indicate the advantages offered by droplet microfluidic techniques whilst providing a basis for identification of shortcomings and room for improvement. Some of the important issues that frequently come up with droplet microfluidic systems are:

1. **Double encapsulation events:** Two different targets from a heterogeneous pool could end up in the same droplet[216,217]. The frequency of these events are rare and quantified in the work presented by Eastburn *et al.*[216]. This could be prevented by FADS or optical methods[223] ensuring single target per droplet. Alternatively, the initial concentration of the sample could be decreased to even lower the frequency of double encapsulations.

2. **Spontaneous coalescence of droplets:** This occurs usually after thermocycling or due to stray electric field and it might lead to cross-contamination, a highly undesirable consequence. This was intercepted by a pinched flow fractionation (size) based droplet sorting[224] after reinjection of the emulsion in the works by Fallah-Araghi *et al.*[213] and Lan *et al.*[220]. Lim *et al.*[217] used shielding electrodes to prevent unwanted electric field related coalescence. Pekin and Taly[222] suggest adding Bovine Serum Albumine (BSA) to limit unwanted coalescence as well as making sure to keep air bubbles away from droplets during collection, thermocycling and reinjection steps.

3. **Molecular transport across droplets:** Small molecules, especially organic ones such as drugs, inside droplets can diffuse out into the surrounding medium and back into adjacent droplets in the emulsion over time[225–227]. While the time scales of molecular transport are usually much longer than that of experiments, this is an important factor to consider specifically with drug screening studies. In order to minimise cross-droplet talk, droplet spacing is an easy and efficient method to implement[227] as well as the introduction of BSA in the aqueous phase[225,226].

5 Conclusion and Outlook

Droplet microfluidics offers ample improvements to conventional screening techniques by reducing sample volumes by a few orders of magnitude and offering high throughput. Extremely laborious methods such as growing monoclonal cultures or processes that are governed by dominant species like highly persistent bacteria or fast growing cells could benefit from droplet microfluidics where isolating single and rare specimens is inherent. By creating minuscule reaction chambers, the effective concentration of samples increases as well as the signal to noise ratios, making it easier to detect targets at low concentrations such as circulating tumour cells. Although promising, many challenges are yet to be addressed for the transition to μHTS; seamless formation of a combinatorial library and robust droplet control technologies that are cross compatible.

In this review, we focussed on the engineering aspect of droplet microfluidic technologies developed for or applicable to screening studies. There's a rejuvenated interest in this field

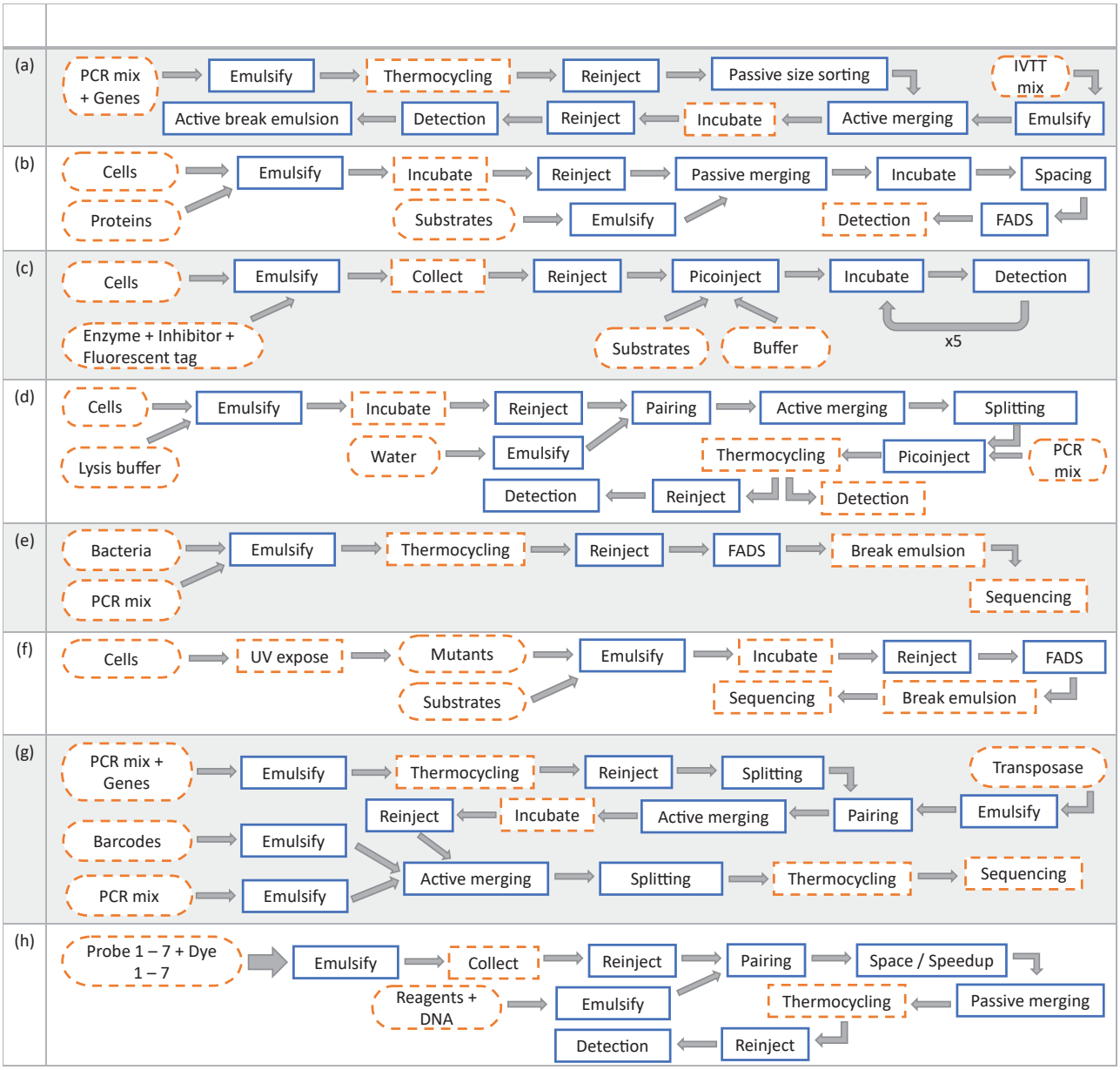

Fig. 15 Workflows for droplet microfluidic systems. Rounded rectangles are for chemicals whereas sharp cornered rectangles show processes. Off-chip events are surrounded by dashed orange while on-chip ones are solid blue line. The title of the presented paper is given in this caption. (a) "A completely in vitro ultrahigh-throughput droplet-based microfluidic screening system for protein engineering and directed evolution"[213]. (b) "Functional single-cell hybridoma screening using droplet-based microfluidics"[214]. (c) "Multiplex analysis of enzyme kinetics and inhibition by droplet microfluidics using picoinjectors"[215]. (d) "Ultrahigh-Throughput Mammalian Single-Cell Reverse-Transcriptase Polymerase Chain Reaction in Microfluidic Drops"[216]. (e) "PCR-Activated Cell Sorting for Cultivation-Free Enrichment and Sequencing of Rare Microbes"[217]. (f) "Microfluidic screening and whole-genome sequencing identifies mutations associated with improved protein secretion by yeast"[218]. (g) "Droplet barcoding for massively parallel single-molecule deep sequencing"[220]. (h) "Multiplex Detection of KRAS Mutations Using Passive Droplet Fusion"[222].

evidenced by the latest developments in droplet control technologies covered in this review. The transition from HTS to droplet based systems was envisioned and strongly supported at the beginning of this century, however, realising that it still had a long way to go with many obstacles, research in this area had slowed down towards the end of its first decade. Advancements in droplet sequencing, an influx of microfluidic start-up companies and the widespread usage of microfluidic systems in various specialised screening and other biological/chemical studies proves that we are in the midst of this long awaited microfluidic revolution.

Most of the explored droplet manipulation techniques utilise various actuation methods that could be achieved with specific and usually incompatible fabrication techniques. Due to this fact, they are very specific to what kind of droplet operations they can perform and do not offer much flexibility. Ensuring that proposed designs are easily adoptable, integrable and robust is very important.

This is not to say that custom microfluidic systems will not be required, on the contrary since more researchers from various disciplines are moving into the field but countless exhaustive studies that carry out the same task over and over again in the search for the right concentration or chemical can significantly benefit from versatile lab on a chip (LOC) platforms capable of carrying out multi-purpose assays. For this reason, restraining from imposing restrictive flow characteristics (i.e specific inlet or outlet pressure) or specific fabrication techniques ensures cross-compatibility so that all the developed methods could be mixed and matched like LEGO® blocks to build a system suiting every specific studies' needs. A passive "plug-n-play" modular microfluidic system, SmartBuild [228], has been developed with similar qualities and it can be upgraded with active manipulation capabilities. Similar platforms utilising various actuation techniques are required for improving these technologies so that the transition to μHTS is accelerated and smoothed.

6 Acknowledgements

The authors would like to thank the reviewers for their valuable suggestions which improved this review significantly. M.S acknowledges help from his dear wife, Ozge Sesen, who designed figure 15 and provided immense moral support.

References

1 B. Bruijns, A. van Asten, R. Tiggelaar and H. Gardeniers, *Biosensors*, 2016, **6**, 41.
2 D. M. Cate, J. A. Adkins, J. Mettakoonpitak and C. S. Henry, *Analytical chemistry*, 2014, **87**, 19–41.
3 D. T. Chiu, D. Di Carlo, P. S. Doyle, C. Hansen, R. M. Maceiczyk, R. C. Wootton *et al.*, *Chem*, 2017, **2**, 201–223.
4 J. D. Caplin, N. G. Granados, M. R. James, R. Montazami and N. Hashemi, *Advanced healthcare materials*, 2015, **4**, 1426–1450.
5 F. Zheng, F. Fu, Y. Cheng, C. Wang, Y. Zhao and Z. Gu, *Small*, 2016, **12**, 2253–2282.
6 B. Xiong, K. Ren, Y. Shu, Y. Chen, B. Shen and H. Wu, *Advanced materials*, 2014, **26**, 5525–5532.
7 P. C. Blainey, *FEMS microbiology reviews*, 2013, **37**, 407–427.
8 A. M. Streets, X. Zhang, C. Cao, Y. Pang, X. Wu, L. Xiong, L. Yang, Y. Fu, L. Zhao and F. Tang, *Proceedings of the National Academy of Sciences*, 2014, **111**, 7048–7053.
9 J. C. Jokerst, J. M. Emory and C. S. Henry, *Analyst*, 2012, **137**, 24–34.
10 C. D. M. Campos and J. A. F. da Silva, *RSC Advances*, 2013, **3**, 18216–18227.
11 H. Bridle, B. Miller and M. P. Y. Desmulliez, *water research*, 2014, **55**, 256–271.
12 M. F. Mora, A. M. Stockton and P. A. Willis, *Electrophoresis*, 2012, **33**, 2624–2638.
13 D. Sinton, *Lab on a Chip*, 2014, **14**, 3127–3134.
14 S. Lee, B. Srinivasan, S. Vemulapati, S. Mehta and D. Erickson, *Lab on a Chip*, 2016, **16**, 2408–2417.
15 B. Srinivasan, S. Lee, D. Erickson and S. Mehta, *Current Opinion in Biotechnology*, 2017, **44**, 103–108.
16 E. M. Wasson, T. A. Douglas and R. V. Davalos, in *Microfluidic Methods for Molecular Biology*, Springer, 2016, pp. 253–294.
17 K. S. Elvira, X. C. i Solvas, R. C. Wootton *et al.*, *Nature chemistry*, 2013, **5**, 905–915.
18 T. Rodrigues, P. Schneider and G. Schneider, *Angewandte Chemie International Edition*, 2014, **53**, 5750–5758.
19 J. de Jong, R. G. H. Lammertink and M. Wessling, *Lab Chip*, 2006, **6**, 1125–1139.
20 X. Chen and J. Shen, *Journal of Chemical Technology & Biotechnology*, 2017, **92**, 271–282.
21 M. Tang, G. Wang, S.-K. Kong and H.-P. Ho, *Micromachines*, 2016, **7**, 26.
22 B. D. Iverson and S. V. Garimella, *Microfluidics and nanofluidics*, 2008, **5**, 145–174.
23 P. Sajeesh and A. K. Sen, *Microfluidics and nanofluidics*, 2014, **17**, 1–52.
24 I. V. Shields, C. Wyatt, C. D. Reyes and G. P. Lpez, *Lab on a Chip*, 2015, **15**, 1230–1249.
25 J. Friend and L. Y. Yeo, *Rev. Mod. Phys.*, 2011, **83**, 647–704.
26 H. Bruus and J. T. Karlsen, *The Journal of the Acoustical Society of America*, 2016, **139**, 2071–2072.
27 A. Neild, *Nature*, 2016, **537**, 493–494.
28 Y. Zhang and N.-T. Nguyen, *Lab on a Chip*, 2017, **17**, 994–1008.
29 C. Zhang, K. Khoshmanesh, A. Mitchell and K. Kalantar-zadeh, *Analytical and Bioanalytical Chemistry*, 2010, **396**, 401–420.
30 K. Khoshmanesh, S. Nahavandi, S. Baratchi, A. Mitchell and K. Kalantar-zadeh, *Biosensors and Bioelectronics*, 2011, **26**, 1800 – 1814.
31 J. Zhang, S. Yan, D. Yuan, G. Alici, N.-T. Nguyen, M. E. Warkiani and W. Li, *Lab on a Chip*, 2016, **16**, 10–34.
32 J. McGrath, M. Jimenez and H. Bridle, *Lab on a Chip*, 2014, **14**, 4139–4158.
33 E. K. Sackmann, A. L. Fulton and D. J. Beebe, *Nature*, 2014, **507**, 181–189.
34 S. M. Prakadan, A. K. Shalek and D. A. Weitz, *Nat Rev Genet*, 2017, **advance online publication**, year.
35 L. R. Volpatti and A. K. Yetisen, *Trends in biotechnology*, 2014, **32**, 347–350.
36 S. K. Vashist, P. B. Luppa, L. Y. Yeo, A. Ozcan and J. H. T. Luong, *Trends in biotechnology*, 2015, **33**, 692–705.

37 I. Kobayashi, K. Uemura and M. Nakajima, *Colloids and Surfaces A: Physicochemical and Engineering Aspects*, 2007, **296**, 285–289.

38 J.-u. Shim, R. T. Ranasinghe, C. A. Smith, S. M. Ibrahim, F. Hollfelder, W. T. Huck, D. Klenerman and C. Abell, *Acs Nano*, 2013, **7**, 5955–5964.

39 B. Zheng, C. J. Gerdts and R. F. Ismagilov, *Current Opinion in Structural Biology*, 2005, **15**, 548–55.

40 J.-U. Shim, G. Cristobal, D. R. Link, T. Thorsen and S. Fraden, *Crystal Growth & Design*, 2007, **7**, 2192–2194.

41 S. Vyawahare, A. D. Griffiths and C. A. Merten, *Chemistry & Biology*, 2010, **17**, 1052–1065.

42 A. B. Theberge, F. Courtois, Y. Schaerli, M. Fischlechner, C. Abell, F. Hollfelder and W. T. S. Huck, *Angewandte Chemie International Edition*, 2010, **49**, 5846–5868.

43 A. Abou-Hassan, O. Sandre and V. Cabuil, *Angewandte Chemie International Edition*, 2010, **49**, 6268–6286.

44 M. T. Guo, A. Rotem, J. A. Heyman and D. A. Weitz, *Lab Chip*, 2012, **12**, 2146–2155.

45 N. Shembekar, C. Chaipan, R. Utharala and C. A. Merten, *Lab on a Chip*, 2016, **16**, 1314–1331.

46 C. Holtze, A. C. Rowat, J. J. Agresti, J. B. Hutchison, F. E. Angile, C. H. J. Schmitz, S. Koster, H. Duan, K. J. Humphry, R. A. Scanga, J. S. Johnson, D. Pisignano and D. A. Weitz, *Lab Chip*, 2008, **8**, 1632–1639.

47 A. R. Abate, C.-H. Chen, J. J. Agresti and D. A. Weitz, *Lab Chip*, 2009, **9**, 2628–2631.

48 J. F. Edd, D. Di Carlo, K. J. Humphry, S. Koster, D. Irimia, D. A. Weitz and M. Toner, *Lab Chip*, 2008, **8**, 1262–1264.

49 E. W. M. Kemna, R. M. Schoeman, F. Wolbers, I. Vermes, D. A. Weitz and A. Van Den Berg, *Lab on a Chip*, 2012, **12**, 2881–2887.

50 D. J. Collins, A. Neild, A.-Q. Liu, Y. Ai *et al.*, *Lab on a Chip*, 2015, **15**, 3439–3459.

51 X. Liu, R. Painter, K. Enesa, D. Holmes, G. Whyte, C. Garlisi, F. Monsma, M. Rehak, F. Craig and C. Smith, *Lab on a Chip*, 2016, **16**, 1636–1643.

52 S. L. Sjostrom, Y. Bai, M. Huang, Z. Liu, J. Nielsen, H. N. Joensson and H. A. Svahn, *Lab on a Chip*, 2014, **14**, 806–813.

53 H. N. Joensson and H. Andersson Svahn, *Angewandte Chemie International Edition*, 2012, **51**, 12176–12192.

54 T. P. Lagus and J. F. Edd, *Journal of Physics D: Applied Physics*, 2013, **46**, 114005.

55 J. J. Burbaum and N. H. Sigal, *Current Opinion in Chemical Biology*, 1997, **1**, 72–78.

56 S. A. Sundberg, *Current Opinion in Biotechnology*, 2000, **11**, 47 – 53.

57 D. L. Chen and R. F. Ismagilov, *Current opinion in chemical biology*, 2006, **10**, 226–231.

58 W. Janzen, in *Molecular Biomethods Handbook*, ed. J. Walker and R. Rapley, Humana Press, 2008, pp. 1097–1118.

59 R. Macarron, M. N. Banks, D. Bojanic, D. J. Burns, D. A. Cirovic, T. Garyantes, D. V. S. Green, R. P. Hertzberg, W. P. Janzen, J. W. Paslay, U. Schopfer and G. S. Sittampalam, *Nat Rev Drug Discov*, 2011, **10**, 188–195.

60 P. Szymański, M. Markowicz and E. Mikiciuk-Olasik, *International Journal of Molecular Sciences*, 2011, **13**, 427–452.

61 S. M. Paul, D. S. Mytelka, C. T. Dunwiddie, C. C. Persinger, B. H. Munos, S. R. Lindborg and A. L. Schacht, *Nat Rev Drug Discov*, 2010, **9**, 203–214.

62 M. Berg, K. Undisz, R. Thiericke, P. Zimmermann, T. Moore and C. Posten, *Journal of Biomolecular Screening*, 2001, **6**, 47–56.

63 R. P. Hertzberg and A. J. Pope, *Current Opinion in Chemical Biology*, 2000, **4**, 445 – 451.

64 C. Ziegenhain, B. Vieth, S. Parekh, B. Reinius, A. Guillaumet-Adkins, M. Smets, H. Leonhardt, H. Heyn, I. Hellmann and W. Enard, *Molecular cell*, 2017, **65**, 631–643.

65 G. X. Y. Zheng, J. M. Terry, P. Belgrader, P. Ryvkin, Z. W. Bent, R. Wilson, S. B. Ziraldo, T. D. Wheeler, G. P. McDermott, J. Zhu, M. T. Gregory, J. Shuga, L. Montesclaros, J. G. Underwood, D. A. Masquelier, S. Y. Nishimura, M. Schnall-Levin, P. W. Wyatt, C. M. Hindson, R. Bharadwaj, A. Wong, K. D. Ness, L. W. Beppu, H. J. Deeg, C. McFarland, K. R. Loeb, W. J. Valente, N. G. Ericson, E. A. Stevens, J. P. Radich, T. S. Mikkelsen, B. J. Hindson and J. H. Bielas, *Nature Communications*, 2017, **8**, 14049.

66 E. Z. Macosko, A. Basu, R. Satija, J. Nemesh, K. Shekhar, M. Goldman, I. Tirosh, A. R. Bialas, N. Kamitaki, E. M. Martersteck *et al.*, *Cell*, 2015, **161**, 1202–1214.

67 P. Neuži, S. Giselbrecht, K. Länge, T. J. Huang and A. Manz, *Nature reviews Drug discovery*, 2012, **11**, 620–632.

68 L. F. Cheow, L. Yobas and D.-L. Kwong, *Applied Physics Letters*, 2007, **90**, 054107.

69 M. J. Fuerstman, P. Garstecki and G. M. Whitesides, *Science*, 2007, **315**, 828–832.

70 M. Prakash and N. Gershenfeld, *Science*, 2007, **315**, 832–835.

71 S. Kou, H. N. Lee, D. van Noort, K. M. K. Swamy, S. H. Kim, J. H. Soh, K.-M. Lee, S.-W. Nam, J. Yoon and S. Park, *Angewandte Chemie*, 2008, **120**, 886–890.

72 A. Abate and D. Weitz, *Small*, 2009, **5**, 2030–2032.

73 J. Yan, W.-A. C. Bauer, M. Fischlechner, F. Hollfelder, C. F. Kaminski and W. T. Huck, *Micromachines*, 2013, **4**, 402–413.

74 S. Li, X. Gong, C. S. Mc Nally, M. Zeng, T. Gaule, C. Anduix-Canto, A. N. Kulak, L. A. Bawazer, M. J. McPherson and F. C. Meldrum, *RSC Advances*, 2016, **6**, 25927–25933.

75 T. Y. Lee, T. M. Choi, T. S. Shim, R. A. Frijns and S.-H. Kim, *Lab on a Chip*, 2016, **16**, 3415–3440.

76 B. F. Silva, C. Rodríguez-Abreu and N. Vilanova, *Current Opinion in Colloid & Interface Science*, 2016, **25**, 98–108.

77 E. Y. Basova and F. Foret, *Analyst*, 2015, **140**, 22–38.

78 W. C. Nelson and C.-J. C. Kim, *Journal of Adhesion Science and Technology*, 2012, **26**, 1747–1771.

79 H.-H. Shen, S.-K. Fan, C.-J. Kim and D.-J. Yao, *Microfluidics and Nanofluidics*, 2014, **16**, 965–987.

80 E. Samiei, M. Tabrizian and M. Hoorfar, *Lab Chip*, 2016, **16**, 2376–2396.

81 S.-Y. Teh, R. Lin, L.-H. Hung and A. P. Lee, *Lab Chip*, 2008, **8**, 198–220.

82 R. Seemann, M. Brinkmann, T. Pfohl and S. Herminghaus, *Reports on Progress in Physics*, 2012, **75**, 016601.

83 A. M. Pit, M. H. Duits and F. Mugele, *Micromachines*, 2015, **6**, 1768–1793.

84 S. Mashaghi, A. Abbaspourrad, D. A. Weitz and A. M. van Oijen, *TrAC Trends in Analytical Chemistry*, 2016, **82**, 118–125.

85 Y. Zhu and Q. Fang, *Analytica chimica acta*, 2013, **787**, 24–35.

86 C. N. Baroud, F. Gallaire and R. Dangla, *Lab Chip*, 2010, **10**, 2032–2045.

87 J.-S. Chen and J.-H. Jiang, *Chinese Journal of Analytical Chemistry*, 2012, **40**, 1293 – 1300.

88 Z. Z. Chong, S. H. Tan, A. M. Gañán-Calvo, S. B. Tor, N. H. Loh and N.-T. Nguyen, *Lab on a Chip*, 2016, **16**, 35–58.

89 H.-D. Xi, H. Zheng, W. Guo, A. M. Gan-Calvo, Y. Ai, C.-W. Tsao, J. Zhou, W. Li, Y. Huang and N.-T. Nguyen, *Lab on a Chip*, 2017, **17**, 751–771.

90 M. Meyer, U. Stenzel, S. Myles, K. Prüfer and M. Hofreiter, *Nucleic Acids Research*, 2007, **35**, e97.

91 Z. Zhu and C. J. Yang, *Accounts of Chemical Research*, 2016.

92 M. Han, X. Gao, J. Z. Su and S. Nie, *Nature biotechnology*, 2001, **19**, 631–635.

93 S.-Q. Gu, Y.-X. Zhang, Y. Zhu, W.-B. Du, B. Yao and Q. Fang, *Analyti-*

cal chemistry, 2011, **83**, 7570–7576.
94 F. Gielen, L. van Vliet, B. T. Koprowski, S. R. A. Devenish, M. Fischlechner, J. B. Edel, X. Niu, A. J. deMello and F. Hollfelder, *Anal. Chem.*, 2013, **85**, 4761–4769.
95 H. Zec, T. D. Rane and T.-H. Wang, *Lab Chip*, 2012, **12**, 3055.
96 M. Sun, S. S. Bithi and S. A. Vanapalli, *Lab Chip*, 2011, **11**, 3949–3952.
97 X. Niu, F. Gielen, J. B. Edel and A. J. deMello, *Nat Chem*, 2011, **3**, 437–442.
98 D.-K. Kang, X. Gong, S. Cho, J.-y. Kim, J. B. Edel, S.-I. Chang, J. Choo and A. J. deMello, *Analytical Chemistry*, 2015, **87**, 10770–10778.
99 A. B. Theberge, E. Mayot, A. El Harrak, F. Kleinschmidt, W. T. S. Huck and A. D. Griffiths, *Lab Chip*, 2012, **12**, 1320–1326.
100 A. R. Abate, T. Hung, P. Mary, J. J. Agresti and D. A. Weitz, *Proceedings of the National Academy of Sciences*, 2010, **107**, 19163–19166.
101 J. S. Edgar, G. Milne, Y. Zhao, C. P. Pabbati, D. S. W. Lim and D. T. Chiu, *Angewandte Chemie International Edition*, 2009, **48**, 2719–2722.
102 X. Z. Niu, B. Zhang, R. T. Marszalek, O. Ces, J. B. Edel and D. R. Klug, *Chemical Communications*, 2009, 6159–6161.
103 V. Trivedi, A. Doshi, G. K. Kurup, E. Ereifej, P. J. Vandevord and A. S. Basu, *Lab on a Chip*, 2010, **10**, 2433–2442.
104 M. Sesen, C. Devendran, S. Malikides, T. Alan and A. Neild, *Lab Chip*, 2017, **17**, 438–447.
105 K. Leung, H. Zahn, T. Leaver, K. M. Konwar, N. W. Hanson, A. P. Pagé, C.-C. Lo, P. S. Chain, S. J. Hallam and C. L. Hansen, *Proceedings of the National Academy of Sciences*, 2012, **109**, 7665–7670.
106 S. H. Jin, H.-H. Jeong, B. Lee, S. S. Lee and C.-S. Lee, *Lab Chip*, 2015, **15**, 3677–3686.
107 B. J. Hindson, K. D. Ness, D. A. Masquelier, P. Belgrader, N. J. Heredia, A. J. Makarewicz, I. J. Bright, M. Y. Lucero, A. L. Hiddessen and T. C. Legler, *Analytical chemistry*, 2011, **83**, 8604–8610.
108 S. Zeng, B. Li, X. Su, J. Qin and B. Lin, *Lab Chip*, 2009, **9**, 1340–1343.
109 J.-W. Choi, S. Lee, D.-H. Lee, J. Kim and S.-I. Chang, *RSC Advances*, 2014, **4**, 20341–20345.
110 N.-T. Nguyen, T.-H. Ting, Y.-F. Yap, T.-N. Wong, J. C.-K. Chai, W.-L. Ong, J. Zhou, S.-H. Tan and L. Yobas, *Applied Physics Letters*, 2007, **91**, 084102.
111 S.-Y. Park, T.-H. Wu, Y. Chen, M. A. Teitell and P.-Y. Chiou, *Lab Chip*, 2011, **11**, 1010–1012.
112 L. Schmid and T. Franke, *Lab Chip*, 2013, **13**, 1691–1694.
113 D. J. Collins, T. Alan, K. Helmerson and A. Neild, *Lab Chip*, 2013, **13**, 3225–3231.
114 J. Xu and D. Attinger, *Journal of Micromechanics and Microengineering*, 2008, **18**, 065020.
115 T. Thorsen, F. H. Roberts, F. H. Arnold and S. R. Quake, *Physical Review Letters*, 2001, **86**, 4163–4166.
116 P. Garstecki, M. J. Fuerstman, H. A. Stone and G. M. Whitesides, *Lab Chip*, 2006, **6**, 437–446.
117 A. Gupta, S. M. S. Murshed and R. Kumar, *Applied Physics Letters*, 2009, **94**, 164107.
118 H. Liu and Y. Zhang, *Journal of applied physics*, 2009, **106**, 034906.
119 V. van Steijn, C. R. Kleijn and M. T. Kreutzer, *Lab Chip*, 2010, **10**, 2513–2518.
120 M. De Menech, P. Garstecki, F. Jousse and H. Stone, *journal of Fluid Mechanics*, 2008, **595**, 141–161.
121 G. F. Christopher, N. N. Noharuddin, J. A. Taylor and S. L. Anna, *Physical Review E*, 2008, **78**, 036317.
122 V. van Steijn, P. M. Korczyk, L. Derzsi, A. R. Abate, D. A. Weitz and P. Garstecki, *Biomicrofluidics*, 2013, **7**, 024108.
123 J. Nunes, S. Tsai, J. Wan and H. Stone, *Journal of Physics D: Applied Physics*, 2013, **46**, 114002.
124 S. L. Anna, N. Bontoux and H. A. Stone, *Applied Physics Letters*, 2003, **82**, 364–366.
125 R. Dreyfus, P. Tabeling and H. Willaime, *Phys. Rev. Lett.*, 2003, **90**, 144505.
126 C. Cramer, P. Fischer and E. J. Windhab, *Chemical Engineering Science*, 2004, **59**, 3045 – 3058.
127 X. Chen, T. Glawdel, N. Cui and C. L. Ren, *Microfluidics and Nanofluidics*, 2015, **18**, 1341–1353.
128 H. C. Shum, D. Lee, I. Yoon, T. Kodger and D. A. Weitz, *Langmuir*, 2008, **24**, 7651–7653.
129 M. B. Romanowsky, A. R. Abate, A. Rotem, C. Holtze and D. A. Weitz, *Lab Chip*, 2012, **12**, 802–807.
130 S. Sugiura, M. Nakajima, J. Tong, H. Nabetani and M. Seki, *Journal of colloid and interface science*, 2000, **227**, 95–103.
131 S. Sugiura, M. Nakajima, S. Iwamoto and M. Seki, *Langmuir*, 2001, **17**, 5562–5566.
132 R. Dangla, S. C. Kayi and C. N. Baroud, *Proceedings of the National Academy of Sciences*, 2013, **110**, 853–858.
133 E. Amstad, M. Chemama, M. Eggersdorfer, L. R. Arriaga, M. P. Brenner and D. A. Weitz, *Lab on a Chip*, 2016, **16**, 4163–4172.
134 F. Schuler, F. Schwemmer, M. Trotter, S. Wadle, R. Zengerle, F. von Stetten and N. Paust, *Lab on a Chip*, 2015, **15**, 2759–2766.
135 F. Schuler, M. Trotter, M. Geltman, F. Schwemmer, S. Wadle, E. Domnguez-Garrido, M. Lpez, C. Cervera-Acedo, P. Santibez and F. von Stetten, *Lab on a Chip*, 2016, **16**, 208–216.
136 A. R. Abate, M. B. Romanowsky, J. J. Agresti and D. A. Weitz, *Applied Physics Letters*, 2009, **94**, 023503.
137 L. Schmid and T. Franke, *Applied Physics Letters*, 2014, **104**, 133501.
138 J. C. Brenker, D. J. Collins, H. Van Phan, T. Alan and A. Neild, *Lab on a Chip*, 2016, **16**, 1675–1683.
139 D. J. Collins, C. Devendran, Z. Ma, J. W. Ng, A. Neild and Y. Ai, *Science Advances*, 2016, **2**, e1600089.
140 X. Feng, B. Liu, J. Li and X. Liu, *Mass spectrometry reviews*, 2015, **34**, 535–557.
141 A. Oedit, P. Vulto, R. Ramautar, P. W. Lindenburg and T. Hankemeier, *Current opinion in biotechnology*, 2015, **31**, 79–85.
142 I. J. Jahn, O. ukovskaja, X.-S. Zheng, K. Weber, T. W. Bocklitz, D. Cialla-May and J. Popp, *Analyst*, 2017.
143 C. M. Ouimet, C. I. DAmico and R. T. Kennedy, *Expert Opinion on Drug Discovery*, 2017.
144 S. Jakiela, S. Makulska, P. M. Korczyk and P. Garstecki, *Lab Chip*, 2011, **11**, 3603.
145 N.-T. Nguyen, S. Lassemono and F. A. Chollet, *Sensors and Actuators B: Chemical*, 2006, **117**, 431–436.
146 M. R. de Saint Vincent, S. Cassagnere, J. Plantard and J.-P. Delville, *Microfluidics and Nanofluidics*, 2012, **13**, 261–271.
147 J.-C. Baret, O. J. Miller, V. Taly, M. Ryckelynck, A. El-Harrak, L. Frenz, C. Rick, M. L. Samuels, J. B. Hutchison, J. J. Agresti, D. R. Link, D. A. Weitz and A. D. Griffiths, *Lab Chip*, 2009, **9**, 1850–1858.
148 M. Srisa-Art, A. J. deMello and J. B. Edel, *Chemical Communications*, 2009, 6548.
149 M. C. Cole and P. J. Kenis, *Sensors and Actuators B: Chemical*, 2009, **136**, 350–358.
150 E. Moiseeva, A. Fletcher and C. Harnett, *Sensors and Actuators B: Chemical*, 2011, **155**, 408–414.
151 X. Niu, M. Zhang, S. Peng, W. Wen and P. Sheng, *Biomicrofluidics*, 2007, **1**, 044101.
152 C. Elbuken, T. Glawdel, D. Chan and C. L. Ren, *Sensors and Actuators A: Physical*, 2011, **171**, 55–62.
153 J. Li, Y. Wang, E. Dong and H. Chen, *Lab Chip*, 2014, **14**, 860.
154 P. K. Isgor, M. Marcali, M. Keser and C. Elbuken, *Sensors and Actuators B: Chemical*, 2015, **210**, 669–675.
155 E. W. Kemna, L. I. Segerink, F. Wolbers, I. Vermes and A. van den Berg, *Analyst*, 2013, **138**, 4585–4592.

156 G. Yesiloz, M. S. Boybay and C. L. Ren, *Lab Chip*, 2015, **15**, 4008–4019.

157 G. Yesiloz, M. S. Boybay and C. L. Ren, *Analytical chemistry*, 2017, **89**, 1978–1984.

158 D. Issadore, K. J. Humphry, K. A. Brown, L. Sandberg, D. A. Weitz and R. M. Westervelt, *Lab on a Chip*, 2009, **9**, 1701–1706.

159 M. S. Boybay, A. Jiao, T. Glawdel and C. L. Ren, *Lab on a Chip*, 2013, **13**, 3840–3846.

160 M. S. Boybay and C. L. Ren, *Encyclopedia of Microfluidics and Nanofluidics*, 2015, 2241–2250.

161 D. Wong, G. Yesiloz, M. S. Boybay and C. L. Ren, *Lab on a Chip*, 2016, **16**, 2192–2197.

162 A. Y. Fu, H.-P. Chou, C. Spence, F. H. Arnold and S. R. Quake, *Analytical Chemistry*, 2002, **74**, 2451–2457.

163 T. Franke, A. R. Abate, D. A. Weitz and A. Wixforth, *Lab Chip*, 2009, **9**, 2625–2627.

164 K. Ahn, C. Kerbage, T. P. Hunt, R. M. Westervelt, D. R. Link and D. A. Weitz, *Applied Physics Letters*, 2006, **88**, 024104 –024104–3.

165 J. J. Agresti, E. Antipov, A. R. Abate, K. Ahn, A. C. Rowat, J.-C. Baret, M. Marquez, A. M. Klibanov, A. D. Griffiths and D. A. Weitz, *Proceedings of the National Academy of Sciences*, 2010, **107**, 4004–4009.

166 H. Zhou and S. Yao, *Lab Chip*, 2013, **13**, 962–969.

167 D. R. Link, E. Grasland-Mongrain, A. Duri, F. Sarrazin, Z. Cheng, G. Cristobal, M. Marquez and D. A. Weitz, *Angewandte Chemie International Edition*, 2006, **45**, 2556–2560.

168 H. Li, Y. Wu, X. Wang, C. Zhu, T. Fu and Y. Ma, *Rsc Advances*, 2016, **6**, 778–785.

169 K. Zhang, Q. Liang, S. Ma, X. Mu, P. Hu, Y. Wang and G. Luo, *Lab on a Chip*, 2009, **9**, 2992–2999.

170 L. Schmid, D. A. Weitz and T. Franke, *Lab on a Chip*, 2014, **14**, 3710–3718.

171 S. Li, X. Ding, F. Guo, Y. Chen, M. I. Lapsley, S.-C. S. Lin, L. Wang, J. P. McCoy, C. E. Cameron and T. J. Huang, *Analytical chemistry*, 2013, **85**, 5468–5474.

172 M. Sesen, T. Alan and A. Neild, *Lab Chip*, 2015, **15**, 3030–3038.

173 I. Leibacher, P. Reichert and J. Dual, *Lab Chip*, 2015, **15**, 2896–2905.

174 H. V. Phan, T. Alan and A. Neild, *Analytical chemistry*, 2016, **88**, 5696–5703.

175 C.-G. Yang, Z.-R. Xu and J.-H. Wang, *TrAC Trends in Analytical Chemistry*, 2010, **29**, 141 – 157.

176 G. M. Whitesides, *Nature*, 2006, **442**, 368–373.

177 S. Feng, L. Yi, L. Zhao-Miao, C. Ren-Tuo and W. Gui-Ren, *Chinese Journal of Analytical Chemistry*, 2015, **43**, 1942–1954.

178 E. Klaseboer, J. P. Chevaillier, C. Gourdon and O. Masbernat, *Journal of Colloid and Interface Science*, 2000, **229**, 274–285.

179 M. Sesen, T. Alan and A. Neild, *Lab Chip*, 2014, **14**, 3325–3333.

180 H. A. Stone, A. D. Stroock and A. Ajdari, *Annu. Rev. Fluid Mech.*, 2004, **36**, 381–411.

181 J.-C. Baret, *Lab on a Chip*, 2012, **12**, 422–433.

182 K. Ahn, J. Agresti, H. Chong, M. Marquez and D. A. Weitz, *Applied Physics Letters*, 2006, **88**, 264105 –264105–3.

183 C. Priest, S. Herminghaus and R. Seemann, *Applied Physics Letters*, 2006, **89**, 134101–134101.

184 M. Mousavichoubeh, M. Ghadiri and M. Shariaty-Niassar, *Chemical Engineering and Processing: Process Intensification*, 2011, **50**, 338 – 344.

185 X. Niu, S. Gulati, J. Edel *et al.*, *Lab Chip*, 2008, **8**, 1837–1841.

186 N. Bremond, A. R. Thiam and J. Bibette, *Phys. Rev. Lett.*, 2008, **100**, 024501.

187 D. H. Yoon, A. Jamshaid, J. Ito, A. Nakahara, D. Tanaka, T. Akitsu, T. Sekiguchi and S. Shoji, *Lab Chip*, 2014, **14**, 3050.

188 S. Lee, H. Kim, D.-J. Won, J. Lee and J. Kim, *Microfluidics and Nanofluidics*, 2016, **20**, 1–9.

189 J. Tullis, C. L. Park and P. Abbyad, *Lab Chip*, 2014, **14**, 3285–3289.

190 M. Chabert, K. D. Dorfman and J.-L. Viovy, *Electrophoresis*, 2005, **26**, 3706–3715.

191 J. S. Eow and M. Ghadiri, *Colloids and Surfaces A: Physicochemical and Engineering Aspects*, 2003, **219**, 253 – 279.

192 J. S. Eow, M. Ghadiri and A. Sharif, *Colloids and Surfaces A: Physicochemical and Engineering Aspects*, 2003, **225**, 193 – 210.

193 P. Atten, L. Lundgaard and G. Berg, *Journal of Electrostatics*, 2006, **64**, 550 – 554.

194 L.-H. Hung, K. M. Choi, W.-Y. Tseng, Y.-C. Tan, K. J. Shea and A. P. Lee, *Lab Chip*, 2006, **6**, 174–178.

195 Y.-C. Tan, Y. Ho and A. Lee, *Microfluidics and Nanofluidics*, 2007, **3**, 495–499.

196 I. Akartuna, D. M. Aubrecht, T. E. Kodger and D. A. Weitz, *Lab on a Chip*, 2015, **15**, 1140–1144.

197 Y.-C. Tan, J. S. Fisher, A. I. Lee, V. Cristini and A. P. Lee, *Lab Chip*, 2004, **4**, 292–298.

198 D. N. Adamson, D. Mustafi, J. X. J. Zhang, B. Zheng and R. F. Ismagilov, *Lab Chip*, 2006, **6**, 1178–1186.

199 D. R. Link, S. L. Anna, D. A. Weitz and H. A. Stone, *Phys. Rev. Lett.*, 2004, **92**, 054503.

200 A. C. Hatch, J. S. Fisher, A. R. Tovar, A. T. Hsieh, R. Lin, S. L. Pentoney, D. L. Yang and A. P. Lee, *Lab Chip*, 2011, **11**, 3838–3845.

201 F. Scheiff, M. Mendorf, D. Agar, N. Reis and M. Mackley, *Lab Chip*, 2011, **11**, 1022–1029.

202 J. H. Jung, G. Destgeer, B. Ha, J. Park and H. J. Sung, *Lab on a Chip*, 2016, **16**, 3235–3243.

203 A. Huebner, D. Bratton, G. Whyte, M. Yang, A. J. deMello, C. Abell and F. Hollfelder, *Lab Chip*, 2009, **9**, 692–698.

204 C. H. Schmitz, A. C. Rowat, S. Köster and D. A. Weitz, *Lab Chip*, 2009, **9**, 44–49.

205 Y. Bai, X. He, D. Liu, S. N. Patil, D. Bratton, A. Huebner, F. Hollfelder, C. Abell and W. T. S. Huck, *Lab Chip*, 2010, **10**, 1281–1285.

206 P. Abbyad, R. Dangla, A. Alexandrou and C. N. Baroud, *Lab Chip*, 2011, **11**, 813–821.

207 E. Fradet, C. Mcdougall, P. Abbyad, R. Dangla, D. Mcgloin and C. N. Baroud, *Lab on a Chip*, 2011, **11**, 4228–4234.

208 W. Wang, C. Yang and C. M. Li, *Lab Chip*, 2009, **9**, 1504–1506.

209 W. Wang, C. Yang, X. Cui, Q. Bao and C. Li, *Microfluidics and Nanofluidics*, 2010, **9**, 1175–1183.

210 R. de Ruiter, A. M. Pit, V. M. de Oliveira, M. H. Duits, D. van den Ende and F. Mugele, *Lab on a Chip*, 2014, **14**, 883–891.

211 J. H. Jung, G. Destgeer, J. Park, H. Ahmed, K. Park and H. J. Sung, *Analytical Chemistry*, 2017, **89**, 2211–2215.

212 R. Zilionis, J. Nainys, A. Veres, V. Savova, D. Zemmour, A. M. Klein and L. Mazutis, *Nat. Protocols*, 2017, **12**, 44–73.

213 A. Fallah-Araghi, J.-C. Baret, M. Ryckelynck and A. D. Griffiths, *Lab on a Chip*, 2012, **12**, 882–891.

214 B. El Debs, R. Utharala, I. V. Balyasnikova, A. D. Griffiths and C. A. Merten, *Proceedings of the National Academy of Sciences*, 2012, **109**, 11570–11575.

215 S. L. Sjostrom, H. N. Joensson and H. A. Svahn, *Lab on a Chip*, 2013, **13**, 1754–1761.

216 D. J. Eastburn, A. Sciambi and A. R. Abate, *Analytical chemistry*, 2013, **85**, 8016–8021.

217 S. W. Lim, T. M. Tran and A. R. Abate, *PloS one*, 2015, **10**, e0113549.

218 M. Huang, Y. Bai, S. L. Sjostrom, B. M. Hallström, Z. Liu, D. Petranovic, M. Uhlén, H. N. Joensson, H. Andersson-Svahn and J. Nielsen, *Proceedings of the National Academy of Sciences*, 2015, **112**, E4689–E4696.

219 D. J. Burgess, *Nat Rev Genet*, 2015, **16**, 376–377.

220 F. Lan, J. R. Haliburton, A. Yuan and A. R. Abate, *Nature Communications*, 2016, **7**, year.
221 D. Pekin, Y. Skhiri, J.-C. Baret, D. Le Corre, L. Mazutis, C. B. Salem, F. Millot, A. El Harrak, J. B. Hutchison and J. W. Larson, *Lab on a chip*, 2011, **11**, 2156–2166.
222 D. Pekin and V. Taly, *Microchip Diagnostics: Methods and Protocols*, 2017, 133–142.
223 Q. Zhang, T. Wang, Q. Zhou, P. Zhang, Y. Gong, H. Gou, J. Xu and B. Ma, *Scientific reports*, 2017, **7**, year.
224 H. Maenaka, M. Yamada, M. Yasuda and M. Seki, *Langmuir*, 2008, **24**, 4405–4410.
225 F. Courtois, L. F. Olguin, G. Whyte, A. B. Theberge, W. T. S. Huck, F. Hollfelder and C. Abell, *Analytical chemistry*, 2009, **81**, 3008–3016.
226 Y. Skhiri, P. Gruner, B. Semin, Q. Brosseau, D. Pekin, L. Mazutis, V. Goust, F. Kleinschmidt, A. El Harrak and J. B. Hutchison, *Soft Matter*, 2012, **8**, 10618–10627.
227 P. Gruner, B. Riechers, B. Semin, J. Lim, A. Johnston, K. Short and J.-C. Baret, *Nature communications*, 2016, **7**, year.
228 P. K. Yuen, *Lab on a Chip*, 2008, **8**, 1374–1378.